



## Article

# Advanced System for Optimizing Electricity Trading and Flow Redirection in Internet of Vehicles Networks Using Flow-DNET and Taylor Social Optimization

Radhika Somakumar <sup>1</sup>, Padmanathan Kasinathan <sup>1,\*</sup>, Rajvikram Madurai Elavarasan <sup>2</sup>  and G. M. Shafiullah <sup>2</sup> 

<sup>1</sup> Department of Electrical and Electronics Engineering, Agni College of Technology, Thalambur, Chennai 600130, Tamil Nadu, India; radhikasomakumar.eee@act.edu.in

<sup>2</sup> School of Engineering and Energy, Murdoch University, Murdoch, WA 6150, Australia

\* Correspondence: padmanathank@act.edu.in or padmanathanindia@gmail.com

**Abstract:** The transportation system has a big impact on daily lifestyle and it is essential to energy transition and decarbonization initiatives. Stabilizing the grid and incorporating sustainable energy sources require technologies like the Internet of Energy (IoE) and Internet of Vehicles (IoV). Electric vehicles (EVs) are essential for cutting emissions and reliance on fossil fuels. According to research on flexible charging methods, allowing EVs to trade electricity can maximize travel distances and efficiently reduce traffic. In order to improve grid efficiency and vehicle coordination, this study suggests an ideal method for energy trading in the Internet of Vehicles (IoV) in which EVs bid for electricity and Road Side Units (RSUs) act as buyers. The Taylor Social Optimization Algorithm (TSOA) is employed for this auction process, focusing on energy and pricing to select the best Charging Station (CS). The TSOA integrates the Taylor series and Social Optimization Algorithm (SOA) to facilitate flow redirection post-trading, evaluating each RSU's redirection factor to identify overloaded or underloaded CSs. The Flow-DNET model determines redirection policies for overloaded CSs. The TSOA + Flow-DNET approach achieved a pricing improvement of 0.816% and a redirection success rate of 0.918, demonstrating its effectiveness in optimizing electricity trading and flow management within the IoV framework.



**Citation:** Somakumar, R.; Kasinathan, P.; Elavarasan, R.M.; Shafiullah, G.M. Advanced System for Optimizing Electricity Trading and Flow Redirection in Internet of Vehicles Networks Using Flow-DNET and Taylor Social Optimization. *Systems* **2024**, *12*, 481. <https://doi.org/10.3390/systems12110481>

Academic Editor: Ed Pohl

Received: 10 August 2024

Revised: 27 September 2024

Accepted: 7 November 2024

Published: 12 November 2024



**Copyright:** © 2024 by the authors. Licensee MDPI, Basel, Switzerland. This article is an open access article distributed under the terms and conditions of the Creative Commons Attribution (CC BY) license (<https://creativecommons.org/licenses/by/4.0/>).

**Keywords:** internet of vehicles; electric vehicles; internet of energy; electricity trading; flow redirection; pricing model

## 1. Introduction

The field of transportation systems research is fast developing, necessitating creative ideas, modeling, and analysis for new advances. Using methodologies and strategies for engineering and supervising these systems across numerous industries, this field applies system approaches to the design, development, and administration of complex systems. In order to improve the functionality and efficiency of transportation systems, key areas include the integration of networking, computing, and physical processes, such as smart grids, IoT systems, and autonomous technologies [1]. The significance of EVs in the energy market can be found in their huge capability to simplify the crisis of fossil fuels and minimize the poisonous emission of gases, which has also acquired the attention of people all over the world. EVs have several benefits, like saving energy, reducing emissions, and preserving the environment. However, the inclusive design of EVs faced several issues. Because of the EV network's mobility and heterogeneity, poor network management may lead to data congestion and overloading of charging ports. As a result, it is important to thoroughly examine the EV network's information and energy management. Meanwhile, the driving ability of EVs is not sturdy enough to fulfil the hopes of vehicular users, which brings specific problems while travelling longer distances. Due to the emergence of EVs, the power grid load can become more apparent. Recently, electricity trading

amongst vehicles has acquired a reliable charging mode, which has also been extensively studied [2]. Based on the benefits of EVs, collaboration amongst vehicles is supposed to be improved to increase driving ability and also effectively prevent the overload issue in power grids [3]. Multiple organizations exist in the IoV, and the transactions are dispersed. As a result, ensuring the security of users' information is a difficult task [4]. The IoV represents an open and combined network model that influences the improved sensing, computation, and communication abilities of its data sources like prediction of traffic [5], RSUs [6], IoT devices, smart city applications [7], planning of routes [8], and management of traffic [9]. By triggering vehicles to mingle with infrastructure and opponent vehicles, the connected vehicle paradigm turns automobiles from tools for mobility into intelligent service platforms. As a result of reducing greenhouse gas emissions from the combustion of petroleum, electrification of transportation is speeding up the commercialization of electric vehicles. This article presents a thorough analysis of the deployment and administration of architectural layers, taking into account the energy flow, data communication, and computing methods and other various aspects.

EVs have attracted universal acknowledgment as a method of offering elevated energy efficiency, low-cost oil usage, and low gas emissions. Nevertheless, the growing acceptance of EVs in the future has created a huge number of energy desires, which also lead to an intrinsic yet complex issue for the providers of a CS of having to maintain effectual services of energy at its CS. For instance, in the unforeseen circumstances of a huge number of EVs immediately requiring to charge their batteries all at once, then their equivalent CSs can face a high energy transmitting cost due to congestion [10,11]. In addition, because of the vibrant energy charging desires from EVs, the CS can face overestimation or underestimation of the energy supply amongst the EVs. Thus, the CS providers need to provide an effectual economic model to increase their profits by attaining cheap energy transfer using dynamic energy desires.

To handle dynamic energy desires and energy efficiency optimization, one requires to precisely forecast the demands of energy from EVs. To predict the energy desires in an EV network, the authors in [12–14] devised machine learning techniques like multiple regression, k-nearest neighbor, deep neural network, shallow neural network, and online reinforcement learning to enhance the demands of the energy prediction accuracy of particular EVs. However, these techniques are not beneficial for a complete EV network as they compute the prediction independently at each CS. It is essential to influence global models or shared information that are used for predicting the energy desires to attain enhanced prediction accuracy amongst the complete network [15].

Connected Electric Vehicles (CEVs) contribute to an improvement in road safety and the reduction in traffic congestion in urban areas. CEVs, or electric vehicles, are of paramount importance in energy markets due to their capacity expansion and adaptable battery models, which enable them to function as mobile power plants. The system possesses the capacity to participate in electricity trading activities in the event that supply stations are offline. The International Energy Agency (IEA) has recorded a considerable quantity of battery-operated electric vehicles (EVs), in the millions. The count is supposed to attain 60 million by 2030. Thus, an elevated penetration of CEVs can make electricity and data exchange a complex process. To handle this process, the ability of CEVs within a smart city has to be devised to promote social welfare and economic problems around the electricity routing and data exchange. The CEV may be a good option for creating workable business plans and streamlining the energy trading process [16]. The road for both data and power decentralization is provided by CEVs' capacity to supplant crucial micro-grid model functions including load balancing, disaster recovery management, and voltage and frequency regulation. The CEV might expedite the shift to a smart electricity paradigm by enhancing societal welfare, increasing profitability, and facilitating auctions. It is very difficult to build an effective energy trading system between nearby nations, nevertheless, given the present power structure. One novel and exciting challenge for preventing RSU congestion and using the least amount of energy possible is flow redirection [17,18].

With this backdrop, the aim of this study is to design an approach for optimal electricity trading and a deep flow redirection mechanism for the IoV using Flow-DNET and TSOA. The four different entities, such as EVs, auctioneers, RSUs, and the IoV server are considered. Energy trading is a mechanism in which different EVs purchase power and RSUs function as auctioneers, receiving and bidding on requests for electricity from EVs. Throughout the auction process, the TSOA optimal trading model is utilized to select the most advantageous CS, with the new objective model factors including the energy and pricing approach also being considered. Once the electricity trading is conducted, the flow redirection is performed. Here, the redirection factor is computed for every RSU in order to decide whether the charging station is overloaded or under loaded. If the CS is overloaded, the Flow-DNET model is utilized for finding the redirection policy. Here, the newly devised TSOA is obtained by integrating Taylor series and SOA.

Figure 1 illustrates the newly devised architecture of the IoV communication network model for EV electricity trading. The centralized cloud server, localized aggregator, cloud-vehicle interface, control and management layer, preprocessing layer, and data processing layer are the essential segments in this architecture.

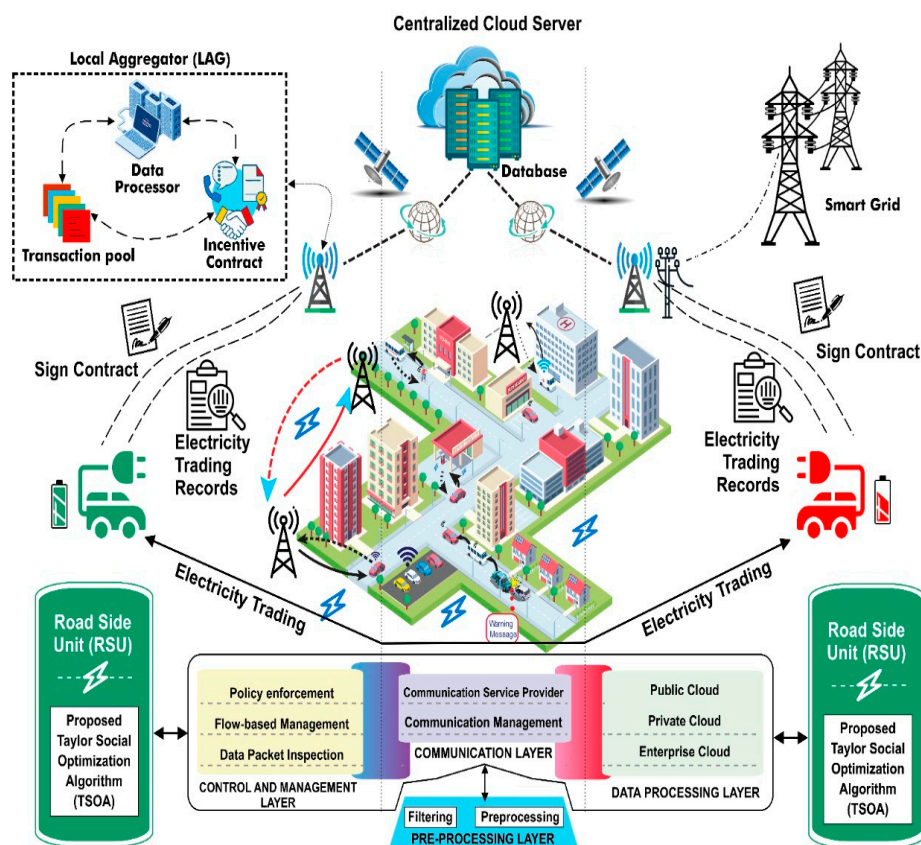


**Figure 1.** System architecture for an IoV communication network for model EVs' electricity trading.

The major contributions of the paper are:

Proposed TSOA for electricity trading:

The electricity trading is performed using TSOA by considering the new objective model, such as energy and the pricing strategy for choosing the best CS. A hybrid of the SOA and Taylor series develops the TSOA.

Motivation:

The huge power accessible with the CS can be taken by EVs for refilling their batteries. The intellectual transportation can assist this by exchanging information regarding the power requirements amongst CS's to EVs and deciding the specific CS for performing

energy trading. This motivates us to devise a new method for energy trading. Various electricity trading and flow redirection techniques are devised in the IoV, and there are several entities contained in the IoV network whose transactions are dispersed. Nevertheless, ensuring information security amongst IoV network consumers is a multifaceted challenge.

The rest of the sections are arranged as follows: Section 2 reveals the review of classical electricity trading and flow redirection techniques in the IoV. Section 3 describes the system of IoV for effective electricity trading. Section 4 displays the proposed model for performing electricity trading. Section 5 discusses the efficiency of the classical model by comparing it with existing techniques. Section 6 offers the conclusion.

## 2. Literature Survey

Automobiles integrate modern devices for the latest Wireless Access Technology (WAT). The apparatus consists of a display screen, numerous application units, a central processing unit, a sensor, an antenna, a camera, radar, and a global positioning system receiver. Their integration as on-board components in vehicles enables vehicular communication, improving affordability, comfort, and safety. Communication devices known as RSUs facilitate communication between on-road vehicles in environments with sparse traffic networks [19,20]. Figure 2 exemplifies various aspects of taxonomy classification on the IoV. As a result of substantial research and technological developments in wireless channel communication, the conventional Intelligent Transport System (ITS) has changed to focus more on vehicle communication. In addition to facilitating communication between on-road vehicles, client applications would have access to a range of WAT to connect to servers situated in smart clouds because of the heterogeneous network environment of the IoV.

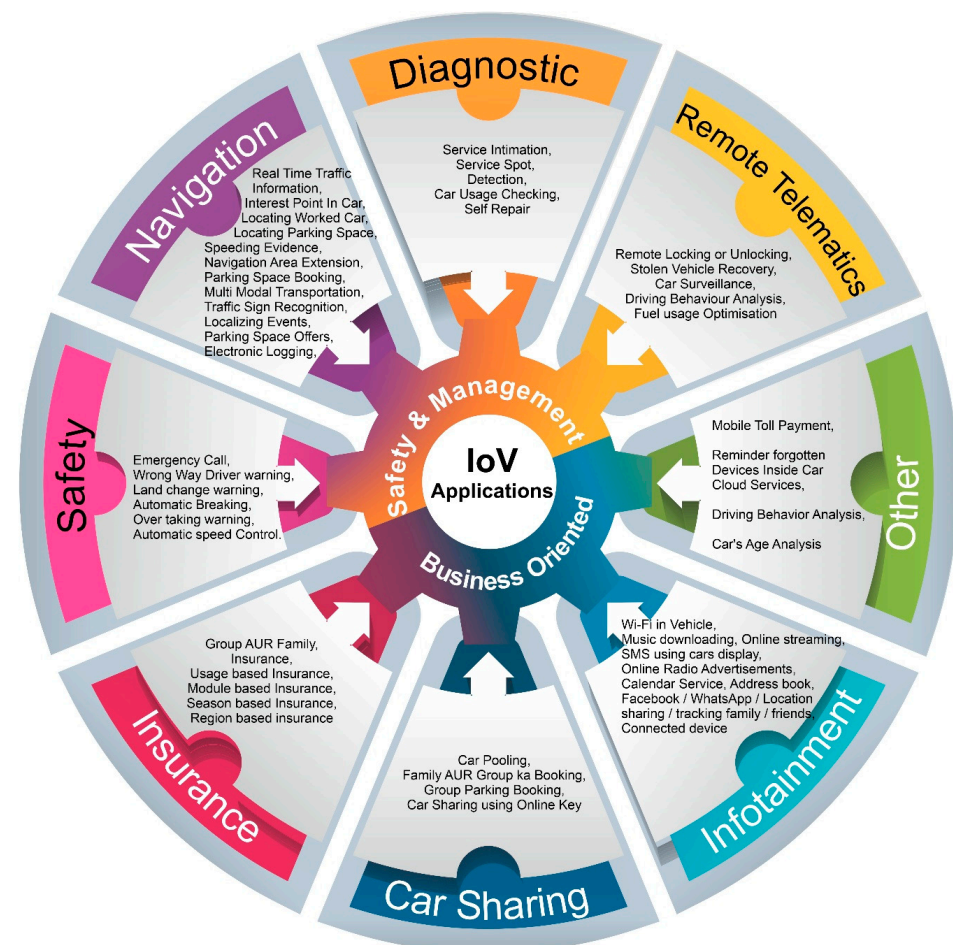


Figure 2. IoV application of taxonomy in various aspects. (Source: O. Kaiwartya et al., 2016) [19].

The five main types of communications between vehicles that make up the IoV communications-based heterogeneous network architecture taxonomy and a heterogeneous network coordination example along with associated services are shown in Figure 3. Implementing a diverse fleet network architecture is a difficult undertaking. V2R, V2V, Vehicles to Sensors (V2S), Vehicles to Personal Devices (V2P), and Vehicles to Infrastructure (V2I) are some of the categories.

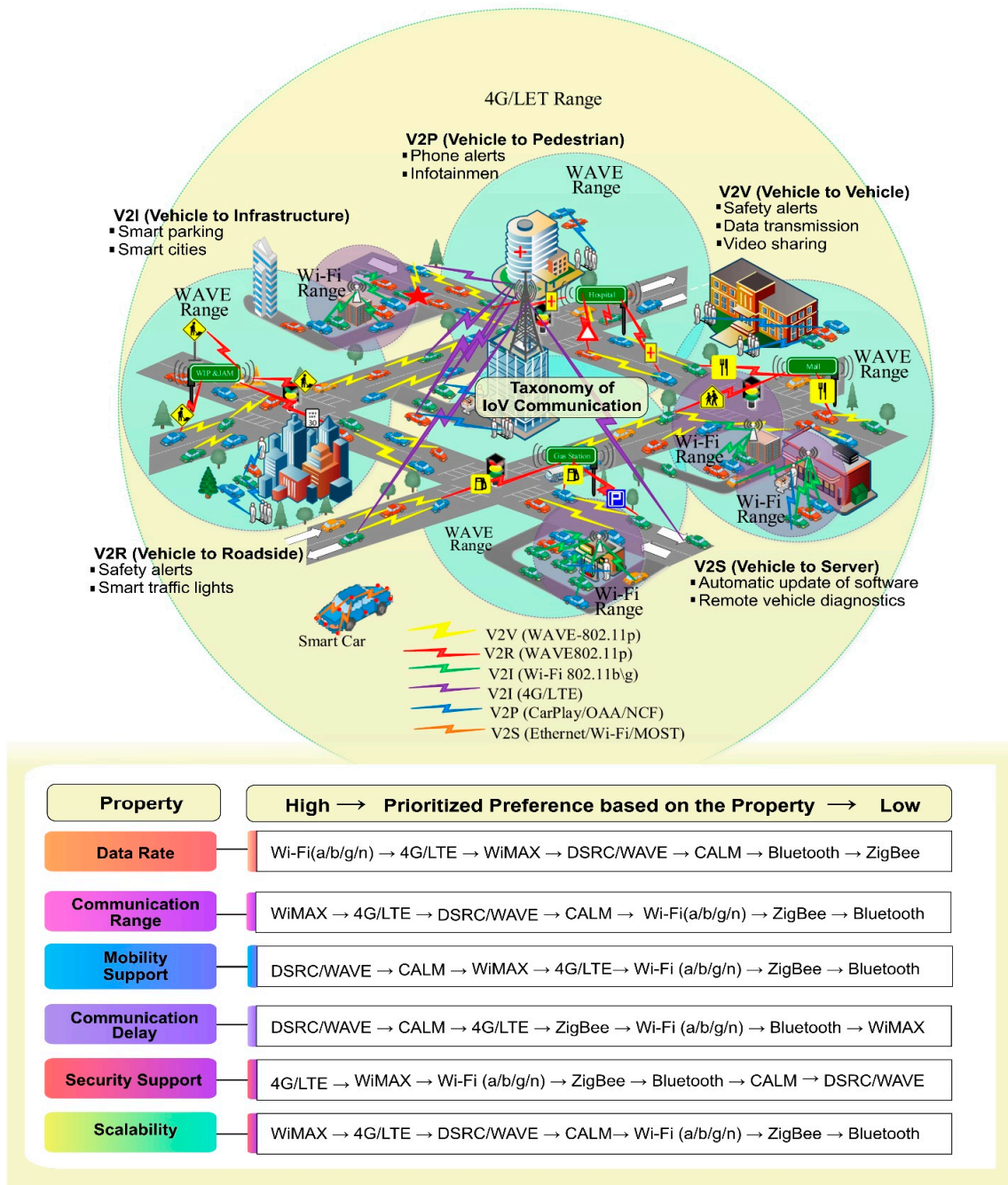


Figure 3. Taxonomy and realization of IoV communication with heterogeneous vehicular networks (Source: Ishita Seth et al., 2022, O. Kaiwartya et al., 2016) [19,21].

A distinct WAT is used to facilitate communication between each IoV car. Additionally, for vehicles and RSUs, various communication devices are part of the communication architecture. Because of the variety of devices included, the design of the IoV’s communication architecture is more complex than that of VANETs, but it still remains focused on

the market. The IoV's heterogeneous vehicular network infrastructure greatly enhances the navigation and supervision of cars. It can offer a dependable framework for online and multimedia applications on the go for a multitude of mobile devices. The following sections emphasize the layered architecture, network concept, benefits, problems, and future elements of the IoV.

The IoE refers to the modernization and automation of electrical infrastructure development between energy producers and consumers. A detailed outline of the framework is provided by [22] along with an amazing explanation of the components and structure of this subsystem for service-oriented management for creating sustainable energy development through the Internet of Everything. There are many benefits to using the IoE, such as increased efficiency, significant cost savings, and a reduction in energy waste. Everything is evolving in the energy market today, including the role of the consumer, the integration of smart technologies, and digitalization. IoV refers to a network of automobiles equipped with middle-tier technology, software, and sensors that allow data transfer and communication over the Internet in accordance with predefined protocols. "VANETs" are a type of mobile ad hoc network that provides communication between automobiles and roadside appliances. It is anticipated that, eventually, the IoV will become an "Internet of autonomous vehicles". One element that is anticipated to support autonomous, connected, electric, and shared (ACES) mobility in the future is the IoV. The authors suggested a distributed multihop task outsourcing decision model to efficiently perform responsibilities. Two primary parts are included in the model: vehicle selection, which finds nearby cars that can be unloaded, and task selection, which finds the best response. The discrete bat approach and greedy algorithm tackle generalized allocation offloading next. The greedy method, sometimes called bat-based strategy, performs better than the scheme where the task vehicle randomly chooses nearby vehicles to transfer in terms of time delay performance, computing power, and task size environment. The aforementioned plan carries out all operations locally [23]. The business model of the energy market is the most needed for research and development, with a particular emphasis on prosumers and consumers' energy trading within local contexts. Figure 4 illustrates the transition from an item-based energy network to a service-based management system. First, the energy internet and management structure have been presented. Next, we examine studies on implementing EV aggregators (AGs) to provide the energy and data infrastructure needed for the IoV. The overview of EV scheduling features both vehicle-to-grid (V2G) and charging scheduling based on the deployed AGs. Additionally, we survey relevant studies on computers and information communication for each scenario.

Figure 5 demonstrates how the electrical system acts as the central facilitator for the connection of different energy transfer networks. Particularly with the increased penetration of renewable energy, the central role of electricity has been reinforced. Furthermore, the electricity network is being created and modified to store the increasing level of renewable energy. This system employs several "power-to-X" conversion technologies to effectively align the supply and demand of renewable energy across extended durations and distances. These technologies include heat-to-liquid, and power-to-gas. Four energy conduits equipped with modern energy conversion technology integrate and coordinate all energy domains, as shown in Figure 6. At the end, it produces a multi-energy system that is affordable and heavily dependent on renewable resources.

### Service-oriented management subsystem

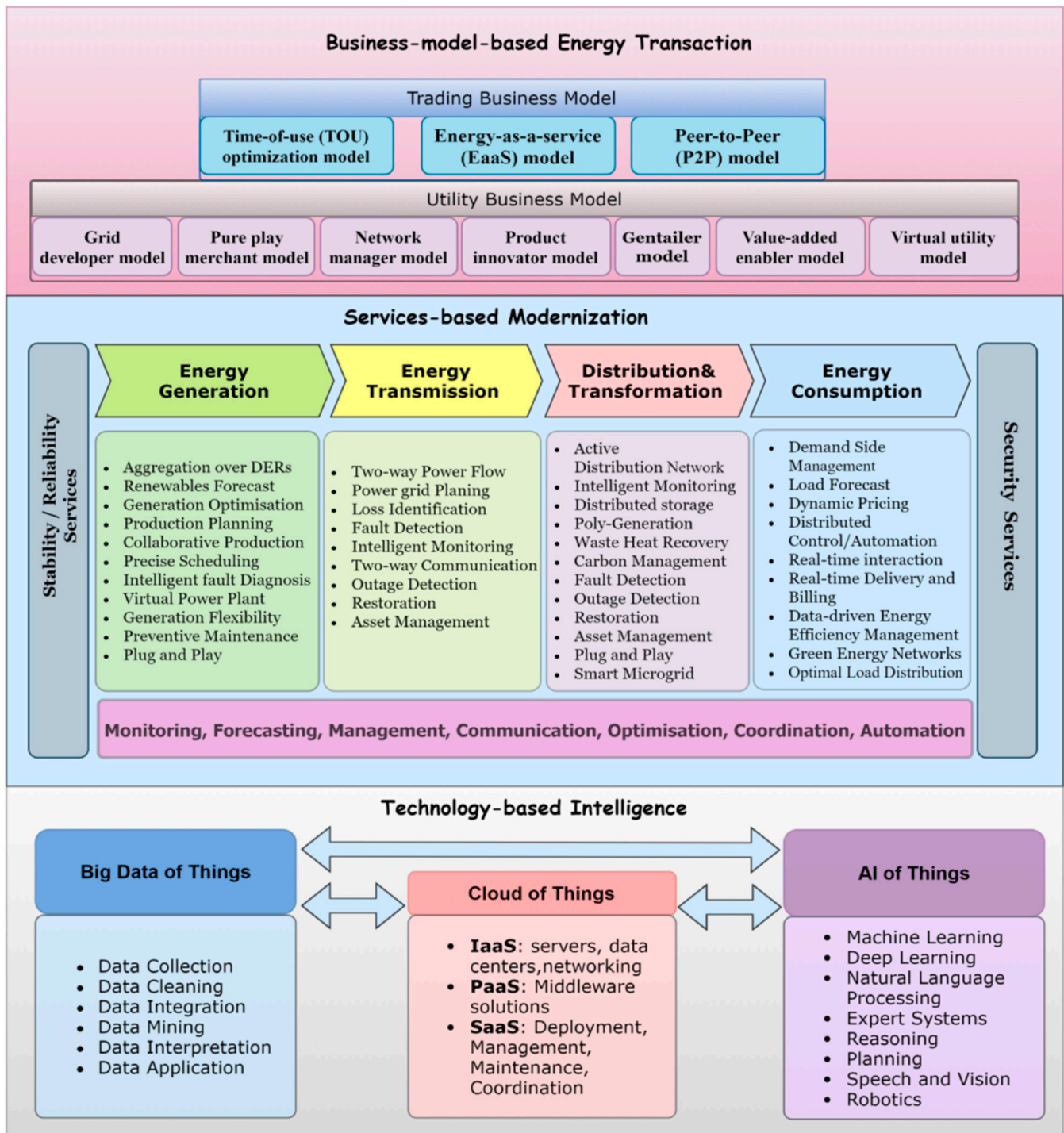


**Figure 4.** Hierarchical integrated energy system enabled with IoV (Source Ying Wu et al., 2021, Elsevier) [22].

The nine classical electricity trading and flow redirection techniques in the IoV are illustrated along with its merits and demerits. Reference [4] developed a V2V electricity trading technique on the basis of Bayesian game pricing using blockchain-assisted IoV. The communication-oriented network subsystem with oriented layers is shown in Figure 7.

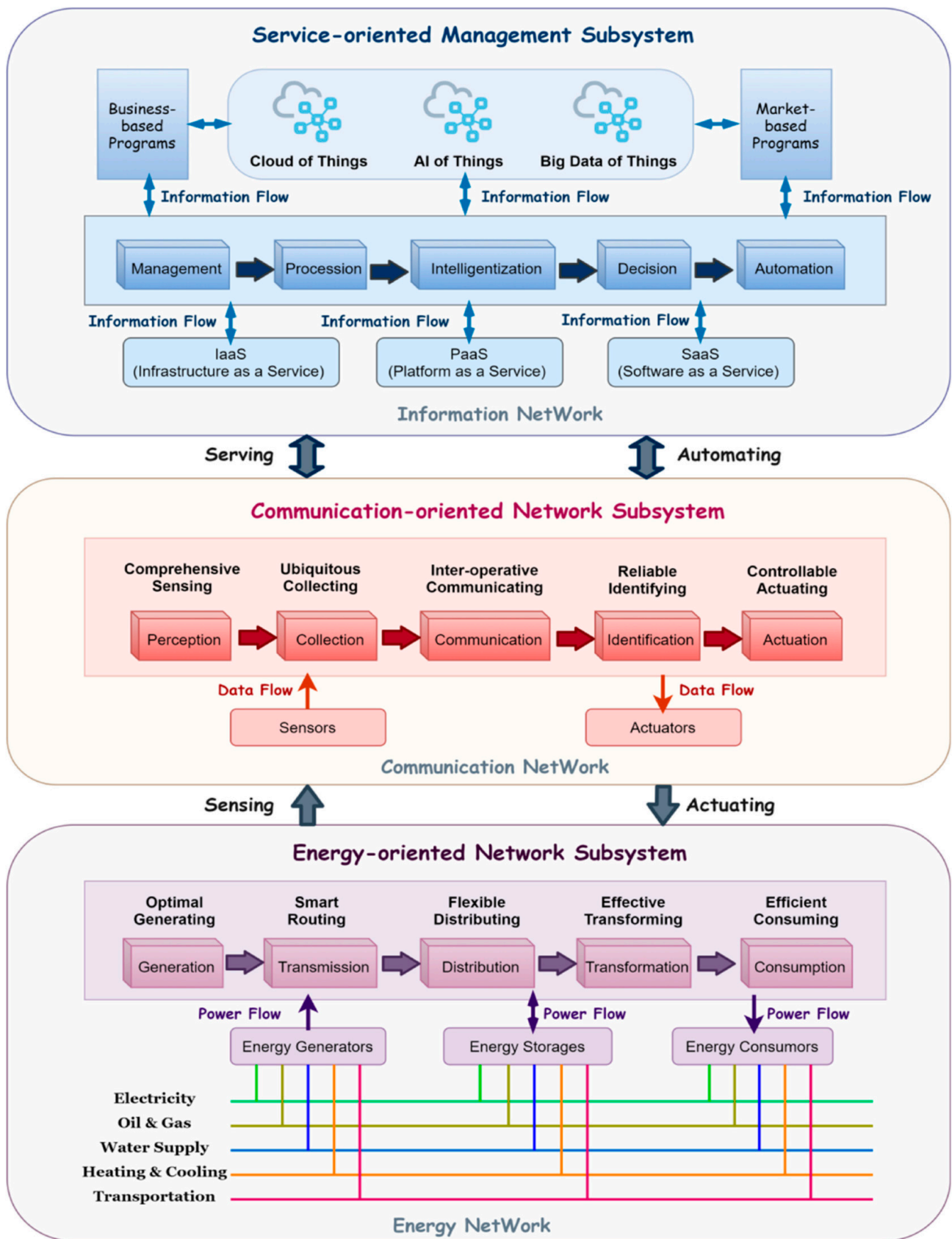
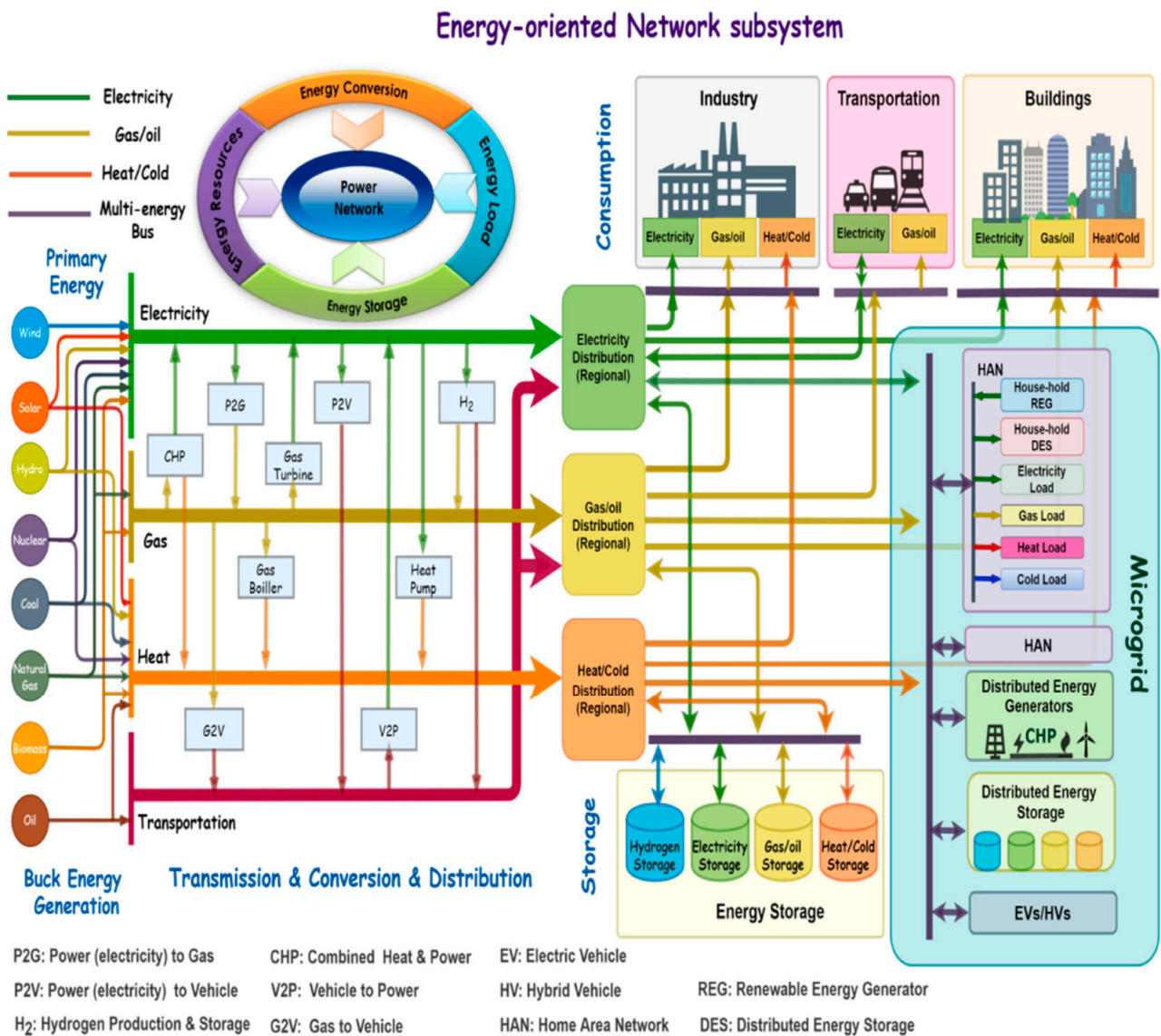


Figure 5. Comprehensive view of EI framework with three subsystems (Source Ying Wu et al., 2021, Elsevier) [22].





**Figure 6.** Essential components comprise the structure and architecture of the energy-focused network system. (Source Ying Wu et al., 2021, Elsevier) [22].

Thereafter, the pricing game was executed by smart contracts. The method was not adapted in order to attain effective outcomes. Reference [17] developed the Decentralized Electricity Trading Framework (DETF) amongst CEVs using consortium blockchain, game theoretic models, and machine learning. We developed a decentralized smart contract system with a stochastic trading mechanism to facilitate CEVs in acquiring and selling electricity in the most lucrative manner. The methodology did not use a comprehensive real-world experimental platform that integrated renewable energy sources with micro-grid architecture. [24] China’s power market effectively establishes incentive agreements and safely trades energy, serving as an example. The digital signature technique ensures the accuracy and dependability of financial transaction data. The energy blockchain technology establishes a decentralized system that ensures data integrity and secure storage. The Practical Byzantine Fault-Tolerant (PBFT) approach ensures the consistency of the data block. The PBFT approach minimizes the time it takes to send data while simultaneously enhancing the process velocity. Penalties for automobiles that violate the restrictions are not included in this approach, and the objective is to enhance stability. In [25], there is a methodology that utilizes electric vehicles (EVs) to effectively control power switching and manipulate the direction of energy flow. In order to address power loss and other

requirements, the CS developed Electric Vehicles as a Service (EVaaS). However, this approach required substantial computational capacity [26]. The intellectual IoV devised a tri-layer transmission system to reduce overall energy consumption and mitigate latency problems. In this instance, we inputted the planning issue into a Deep Reinforcement Learning (DRL) system. Regrettably, the design did not include any optimization strategy to enhance the system's performance [27]. In order to decrease the average reaction time in fog-assisted Internet of Vehicles models, a resilient offloading approach was developed for real-time traffic management. This method was utilized to organize the movement of traffic between fog nodes and address the issue of optimizing offloading in this particular scenario. In [28], a control and regulation technique was devised whose goal was to attain a balanced production or consumption model. However, this technique was not able to optimize the available state of charge (SoC). For the energy-efficient task offloading, [29] devised UAV-CCIO, or UAV-Enabled Computing and Communications Intelligent Offloading. The UAV consumed less energy and travels less distance without routing; therefore, it uses no energy. In [30], the authors developed a consortium blockchain to minimize dependence on trusted third parties. In addition, the PBFT algorithm was incorporated with the consensus algorithm to minimize resource consumption and improve consensus efficiency. However, the system's reliability was affected because of the interference of bad nodes. In [31], the suitable charging station for electric vehicles was determined by scheduling the charging points using a vehicle ad hoc network. Fake security concerns and environmental changes may delay and expend data. To save computer power and identify hazards, automated anomaly detection was devised in [32]. In [33], the authors proposed an algorithm for finding the optimal charging station for EVs using the proposed sailfish optimization algorithm. This method utilized only a single optimization for finding the CS. In order to optimize the finding of a CS, the development of a hybrid optimization technique will provide a better solution. In [34], the authors present an energy-aware optimization (EAO) technique for improving CAEV energy efficiency by taking into account the vehicle traffic nexus. Moreover, this method developed a torque monitoring management approach to control and maintain the electric powertrain for optimal efficiency. The authors proposed an improved MRNN classifier and 2CKECC method in [35] to forecast IoV vehicular mobility, security, and content caching. Although the energy consumption of this method was low, this method utilized more steps to execute it. Here, an innovative Harris Self-Avoiding Hawks Optimization (HSAHO) was devised to select the relay vehicles (RVs). However, the processing time of this scheme was high. In [36], an efficient EV charging technique was established based on mobile edge computing (MEC). Here, the global controller served as a centralized cloud platform that enabled analytics from a CS and the coordinates of charging reservations for mobile EVs to predict CS availability. The charging performance and communication efficiency of the model was high, but the performance was reduced due to network congestion.

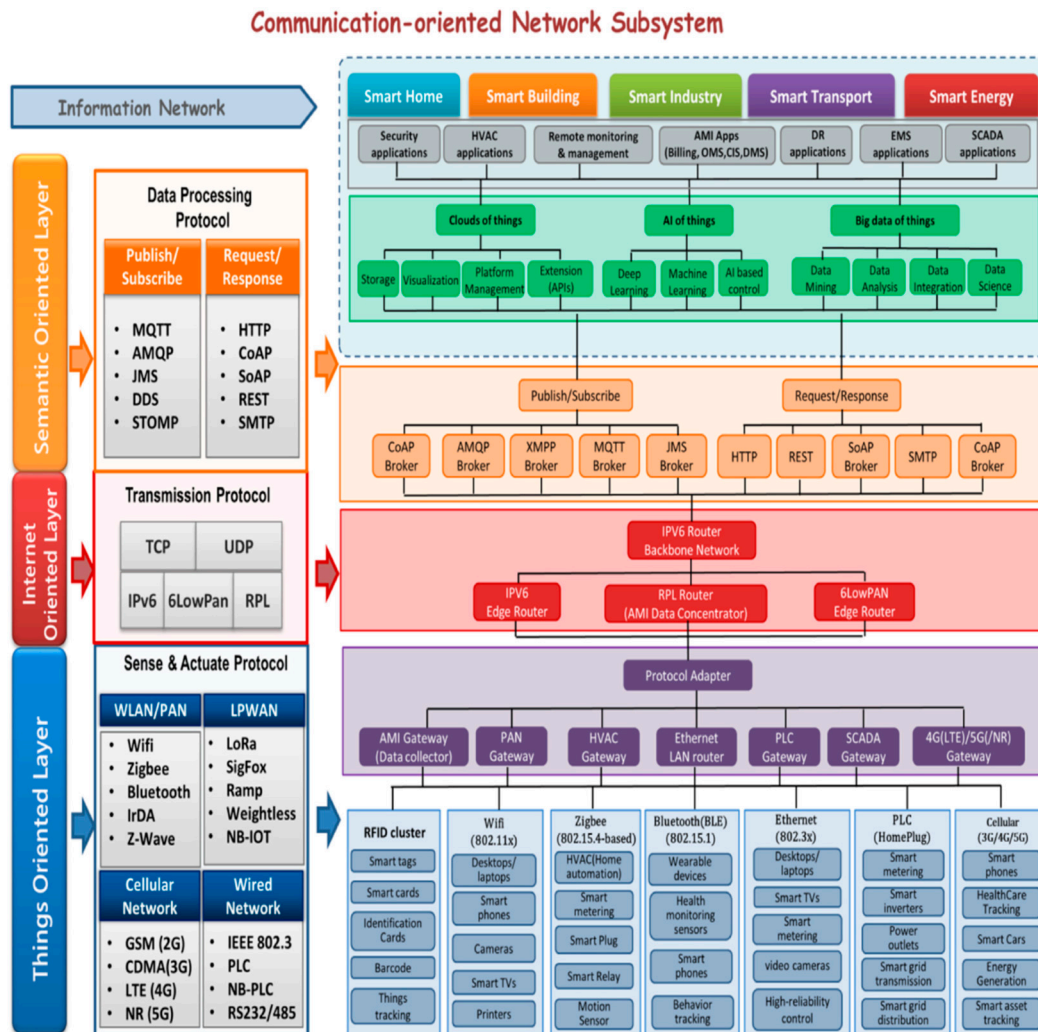


Figure 7. Communication-oriented network architecture and protocols (Source Ying Wu et al., 2021, Elsevier) [22].

### 3. System Model

Electric cars have the potential to enhance road safety and alleviate traffic congestion in cities. The enhanced battery system’s flexibility and capacity of EVs may render them indispensable in the electricity market. Due to its ability to transfer energy internally, it is particularly advantageous in scenarios when power sources are momentarily or entirely unavailable.

Figure 8 illustrates the system paradigm for power trading in the Internet of Things (IoT) system. Consider a city divided into  $d \times d$  blocks, which contains an IoV server, a group of electric vehicles  $\{V_1, V_2, \dots, V_i, \dots, V_p\}$ , and a set of RSUs  $\{r_1, r_2, \dots, r_j, \dots, r_n\}$ . Here, the RSUs act as auctioneers and electric vehicles have bidirectional charging and discharging capabilities. An electrical seller is a self-sufficient vehicle with a specified quantity of energy that may be shared with other buyers or used to power itself. The RSU enables charging and discharging between EVs. Vehicle flow arrival is denoted by RSU  $r_j$  and follows the Poisson process with  $\lambda_j$ .

The notation table is depicted in Table 1.

**Table 1.** Notation table.

Symbol	Definition
$p$	total number of EVs
$n$	number of RSUs
$\lambda_j$	vehicle arrival rate
$SoC_i^{prs}$	present state of $i^{th}$ EV's battery
$SoC_i^{thr}$	SoC threshold value
$SoC_i^{max}$	maximum SoC level of $i^{th}$ EV
$Q^r$	rated battery capacity
$V_t$	terminal voltage
$SoC_l^{max}$	maximum SoC value at $l^{th}$ EV
$SoC_l^{pv}$	SoC of panels
$E_l^{rt}$	rated energy of $l^{th}$ EV
$SoC_l^{prs}$	present state of $V_l$ battery
$SoC_{l \leftarrow i}^{drw}$	energy drawn by $V_l$ from $V_i$
$SoC_{i \rightarrow l}^{gvm}$	SoC given by $V_i$ to $V_l$
$SoC_{i \rightarrow l}^{trw}$	SoC of $V_i$ dissipated while travelling to $V_l$ for charging $E_i^{req}$
$d_x$	distance of $x$ from end of block
$d_y$	distance of $y$ from end of block
$d$	fixed distance of one block
$n_{x \rightarrow y}$	count of blocks present in $x$ to $y$
$P_i^s$	cost
$P_i^b$	price at which EV bought the energy
$g(i, k)$	size of load flows redirected through RSU from $r_i$ to $r_k$
$d_{r_i, r_k}$	unit transmission delay
$t_{i, redirect}^j$	total delay
$a, b$	constant
$E_l^{req}$	energy required by $l^{th}$ EV
$P_i^s$	price announced by $i^{th}$ EV
$d_{i \leftarrow l}$	distance
$p$	total number of EV
$E_l^{rt}$	rated energy of $l^{th}$ EV
$F$	initialization of solution
$\kappa$	Total solution
$F_\rho$	$\rho^{th}$ solution
$rand$	random number
$X$	best position
$Y$	coefficient of personal choice
$F_r^{old}$	old position of entity
$S$	best solution
$A$	density point

Table 1. Cont.

Symbol	Definition
$z_1$	results obtained by member of society
$F_r^k$	Taylor polynomial at current iteration
$F_r^{k'}$	previous iteration Taylor polynomials
$J$	empty point
$\frac{z_l}{\sum_{r=1}^l z_r}$	relative fitness
$z_r$	results obtained by member of society
$X$	number of parked vehicles
$\mu_p$	service rate
$\lambda_j^{vehicle}$	arrival rate of vehicle
$K$	number of EVs processed
$C$	capacity
$d$	distance
$t$	delay
$L$	load
$f_p^1$	$p^{th}$ visible neuron in first RBM
$h_l^1$	$l^{th}$ hidden neuron
$q$	hidden neurons count
$u$ and $v$	biases in visible layer and hidden layer
$u_p^1$	bias linked to $p^{th}$ visible neuron
$v_l^1$	bias linked to $l^{th}$ hidden neuron
$W_{pl}^1$	weight amongst $p^{th}$ visible neuron and $l^{th}$ hidden neuron
$\sigma$	activation function
$\{h_l^1\}$	first RBM output
$W_{ll}^2$	weight amongst $l^{th}$ visible neuron and $l^{th}$ hidden neuron in second RBM
$q \times q$	size of weight vector
$v_l^2$	bias linked to $l^{th}$ hidden neuron
$q$	neurons count in input layer
$M$	hidden neurons
$z$	count of neurons in output layer
$W^I$	weight vector amongst input and hidden layers
$W_{IK}^I$	weight amongst $l^{th}$ input neuron and $K^{th}$ hidden neuron
$X_K$	bias of hidden neuron
$W^H$	weights amongst hidden layer and output layer
$W_{Kr}^H$	weight amongst $K^{th}$ hidden neuron and $r^{th}$ output neuron
$s_K$	hidden layer output

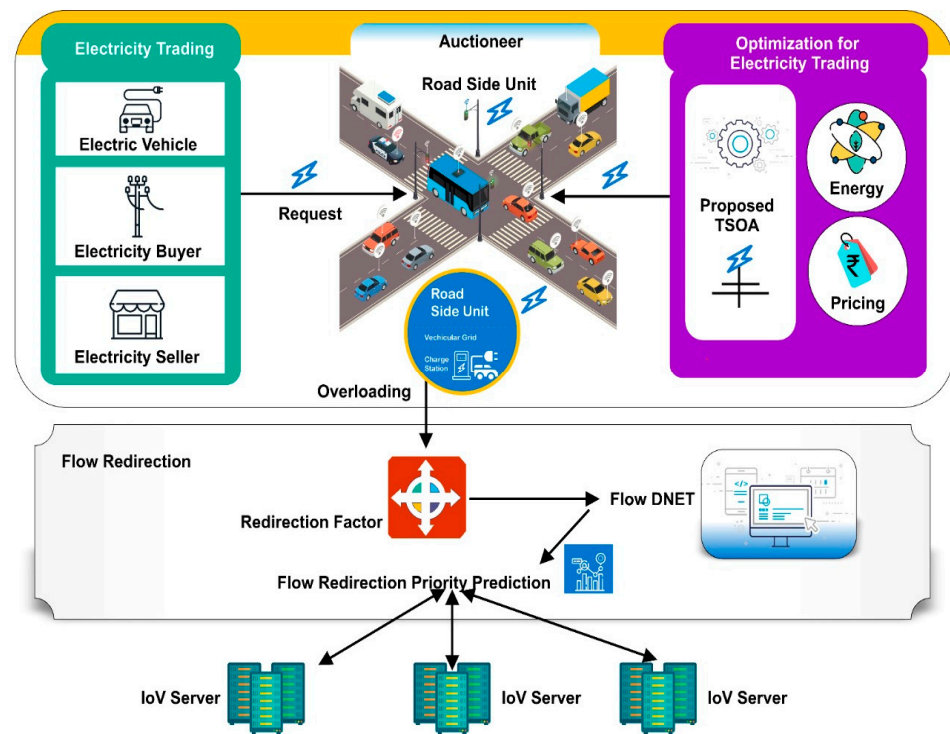


Figure 8. System model of IoV network for electricity trading.

### 3.1. Energy Model

The energy model [25] is discussed below. To develop an effectual electricity trading technique, it is imperative to discover the consumed energy by each EV. Here, the CS proceeds as an energy borrower and the EV reacts as an energy distributor. Thus, every EV should have energy obtainable in its battery to fulfil the desires of the requested charging stations. The quantity of energy with  $i^{th}$  EVs can contribute to the request for a CS based on the threshold value of  $SoC_i^{thr}$ . Thus, the accessible SoC with  $i^{th}$  EV  $SoC_i^{avl}$  can contribute to the requested CS as,

$$SoC_i^{avl} = SoC_i^{prs} - SoC_i^{thr} \quad (1)$$

The energy accessible with  $i^{th}$  EVs ( $E_i^{avl}$ ) can be given to the requested CS and is formulated as,

$$E_i^{avl} = (SoC_i^{prs} - SoC_i^{thr}) E_i^{rt}; \text{ If } SoC_i^{prs} > SoC_i^{thr} \quad (2)$$

$E_i^{rt}$  is the rated energy of  $i^{th}$  EVs and is formulated as,

$$E_i^{rt} = SoC_i^{max} Q^r V_t \quad (3)$$

The remaining energy required to reach  $SoC_i^{max}$  by  $l^{th}$  EVs ( $V_l$ ) as the buyer is given as,

$$SoC_l^{req} = SoC_l^{max} - SoC_l^{pv} \quad (4)$$

The energy required by  $V_l$  to reach  $SoC_l^{max}$  is given by,

$$E_l^{req} = (SoC_l^{max} - SoC_l^{pv}) E_l^{rt} \quad (5)$$

$E_l^{rt}$  is computed similarly to that of  $i^{th}$  EVs.

After charging  $E_l^{req}$  from  $V_l$ , update the SoC, which is given by,

$$SoC_l^{upd} = SoC_l^{pvs} - SoC_{l \leftarrow i}^{drw} \quad (6)$$

After updating the SoC of  $V_i$ ,

$$SoC_i^{upd} = SoC_i^{pvs} - SoC_{i \rightarrow l}^{gvm} - SoC_{i \rightarrow l}^{trv} \quad (7)$$

### 3.2. Mobility Model

The mobility model [25] is stated to exemplify the development of EVs and to compute the alteration in the EV's position considering velocity, acceleration, and location in a particular instance. The whole city is split into several  $d \times d$  blocks to model the mobility of EVs. Each block comprises various EVs and CSs. To maximize earnings and accomplish the most efficient energy exchange, EVs seek to trade with other EVs and charging stations (CSs) in the same block. Nonetheless, they may interchange products and services with any other charging station. The biggest difference between CSs and EVs is the amount of energy they use. We may calculate the distance between the two by determining  $d_{x \rightarrow y}$  where CS is  $y$  and  $x$  using a symbol to indicate the EV's location. The distance between two locations  $x$  and  $y$  is determined by the actual path  $d_{x \rightarrow y}$ , which is calculated based on the Manhattan block design:

$$d_{x \rightarrow y} = \left| \frac{d_x}{d} \right| \times d + \left| \frac{d_y}{d} \right| \times d + n_{x \rightarrow y} \times d \quad (8)$$

The EV computes the distance of each CS and sends these data to the energy trading model that computes the net profit of the EV considering this distance.

### 3.3. Pricing Model

There are two scenarios in which pricing is determined: when an electric vehicle has excess energy available for sale and when a charging station needs to buy energy [25]. Electric vehicle owners have the ability to choose the price at which their cars participate in energy transactions. Batteries power electric vehicles for propulsion. The EVs choose a System on Chip (SoC) to regulate the expenses associated with charging and discharging the battery.

$$P_i^s = \kappa \left( \frac{SoC_i^{\max}}{SoC_i^{avl} - SoC_i^{thr}} \right); \text{ such that } P_i^s > P_i^b \quad (9)$$

$\kappa$  is fixed in such a way that the overall supplying cost is higher compared to the receiving price.

### 3.4. Redirection Model

The redirection model [26] is presented below. To balance the offloading flows of tasks, the RSUs are adapted to be reachable amongst each other. As flows occurring at the RSUs can be different, a high-loaded RSU can redirect flows to a low-loaded RSU. Here, the following constraints must be fulfilled:

$$g(i, k) = \begin{cases} -g(k, i), & i \neq k \\ 0, & \text{Otherwise} \end{cases} \quad (10)$$

Indicators are given by  $i, k \in \{1, 2, \dots, u\}$ . The states of the communication channel are supposed to be equal and kept unaltered during one scheduling time slot. Assume  $d_{r_i, r_k}$  is caused by transmitting offloading tasks amongst RSU  $r_i$  and RSU  $r_k$ . If redirected flow  $g(i, k) < 0$ , the RSU  $r_k$  transmits flow to RSU  $r_i$  and delay  $(-g(i, k) \times d_{r_i, r_k})$  exists.

The  $t_{i, redirect}^j$  produced by redirecting flows from RSU  $i$  to the RSU with time slot  $j$  is evaluated as,

$$t_{i, redirect}^j = \sum_{k=1}^u |\max\{g(i, k), 0\} \times d_{r_i, r_k}| \quad (11)$$

Furthermore, the consumption of the energy of redirection for RSU  $r_i$  at time slot  $j$  is given by  $E_{i,redirect}^j = P_{r_i} \times t_{i,redirect}^j$ . The final arriving task flows at RSU  $r_i$  can be given as,

$$\bar{\lambda}_i = \lambda_i - \sum_{k=1}^u g(i, k) \quad (12)$$

#### 4. Proposed TSOA-Based Flow-DNET for Optimal Electricity Trading

The goal is to design an approach for optimal electricity trading and deep flow redirection mechanisms for the IoV using Flow-DNET and TSOA. Figure 9 represents the schematic view of the optimal electricity trading model in the IoV using the proposed TSOA-based Flow-DNET. Four different entities, such as EVs, auctioneers, RSUs, and IoV servers, are considered. In the energy trading market, electric vehicles (EVs) act as buyers by transmitting power demand to RSUs. After that, an auctioneer may employ RSUs to make it easier for people to place bids on these requests. Finding the best charging station is the job of the auctioneer, who employs the revised goal model that factors in things like energy and pricing strategies. The TSOA optimal trading model serves as the foundation for this choice. The TSOA optimal trading model redirects the current after the power transaction is completed. For every RSU, the TSOA optimal trading model computes the redirection factor to determine if the charging stations are overloaded or underloaded. If a charging station is overloaded, we utilize the Flow-DNET model to find the redirection policy. Here, the Flow-DNET is newly devised using a deep network based on the optimization algorithm, called TSOA. Moreover, the TSOA is obtained by combining the Taylor series [26] and SOA [37].

The different parts of IOV architecture, taxonomy, integrated energy systems, compressive views, essential components, communication-oriented architecture, and system models are all shown in Figure 10. It provides readers with a holistic understanding of the interconnected and integrated nature of the IOV landscape. This visual synthesis brings together diverse elements from the previously explored technologies. Beginning with the “architecture of IOV,” the integrated framework delves into the foundational structures that underpin IOV systems. It extends its reach to include the insights from “taxonomy,” providing a structured classification of IOV components and entities. The figure further explores the “Integrated Energy System for IOV,” demonstrating the interplay between energy considerations and the overall IOV infrastructure.

Moving beyond isolated views, the framework introduces a “Compressive View,” encapsulating a condensed but inclusive representation of the IOV landscape. It then dissects the “Essential Components,” emphasizing the key elements crucial for the functioning of the IOV.

##### 4.1. Electricity Trading

- EVs (EV buyers) send a request to auctioneers.
- The auctioneers broadcast the information to the seller and buyer.
- The trading scheme is based on three conditions and will be executed.
- RSUs provide electricity to buyers.
- If the RSU does not have sufficient energy to sell, it begins trading by finding a suitable seller.
- If the above two conditions fail (OR) and the RSU is overloading, then redirection will be performed.

Figure 11 represents the proposed Taylor Social Optimization model algorithm flow with an optimal solution.

##### 4.1.1. Trading Using Proposed TSOA

The proposed TSOA, which combines the Taylor series and SOA, serves the trading purposes in this context. The subsections provide a comprehensive explanation of the



phases involved in the proposed TSOA, the fitness function, and the method used for solution encoding. The redirection factor is computed by every RSU to determine the charging stations' overload or underload status.

### 1. Solution encoding

The choice of result representation is crucial in determining the optimal solution for optimization problems. To streamline the energy transfer on the Internet of Vehicles, EV providers are selected based on the planned Transmission System Operator Agreement (TSOA). The optimization process begins with an initial value (the solution set) and progresses towards the optimal value. The vendor assignment solution set comprises a group of EV sellers who are enthusiastic about exchanging energy with clients. The solution vector is generated randomly, resulting in a diverse group of EV sellers. The suitability of the solution set then determines the optimal quantity of EV merchants. By using a fitness function, we can ascertain the optimal number of electric vehicle vendors to include in the trading procedure. Figure 12 illustrates the solution representation that utilizes the produced TSOA. Please provide a roster of electric vehicle suppliers who are enthusiastic about doing business in this area.

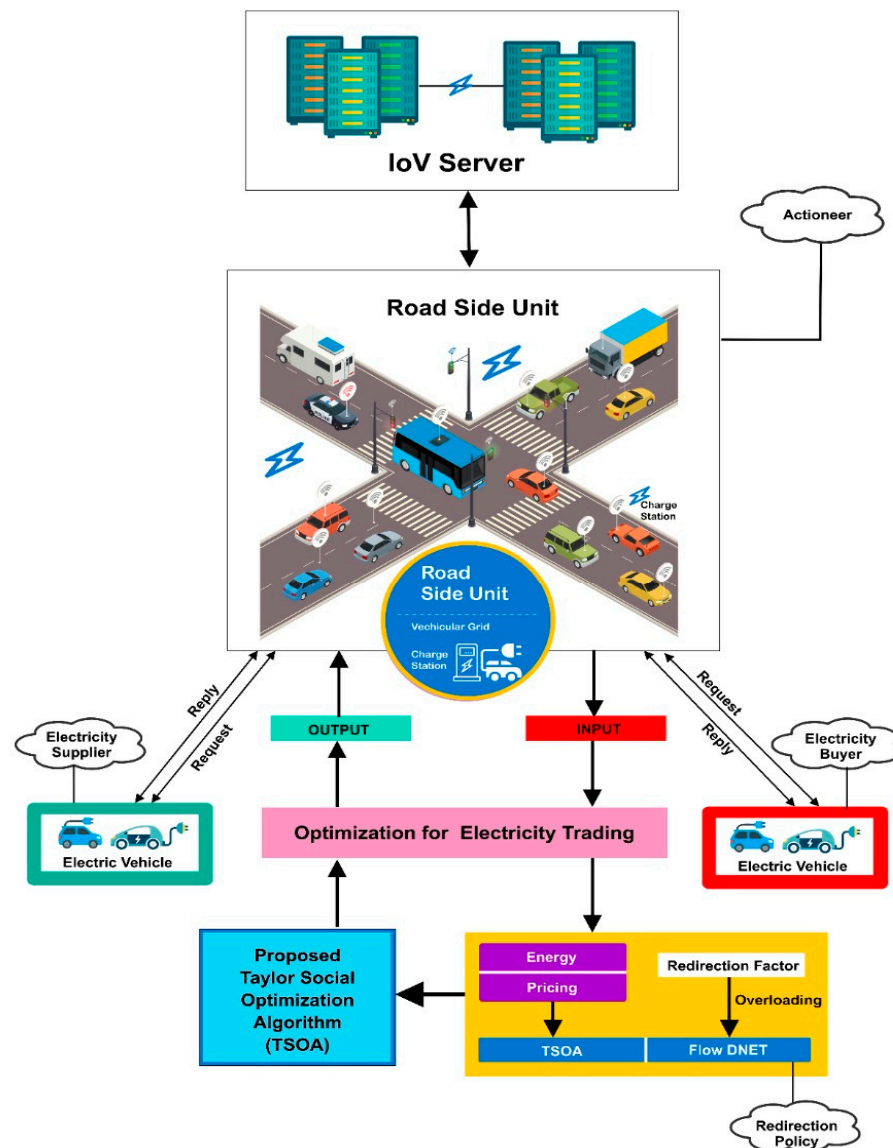


Figure 9. Schematic view of optimal electricity trading model in IoV using proposed TSOA-based Flow-DNET.

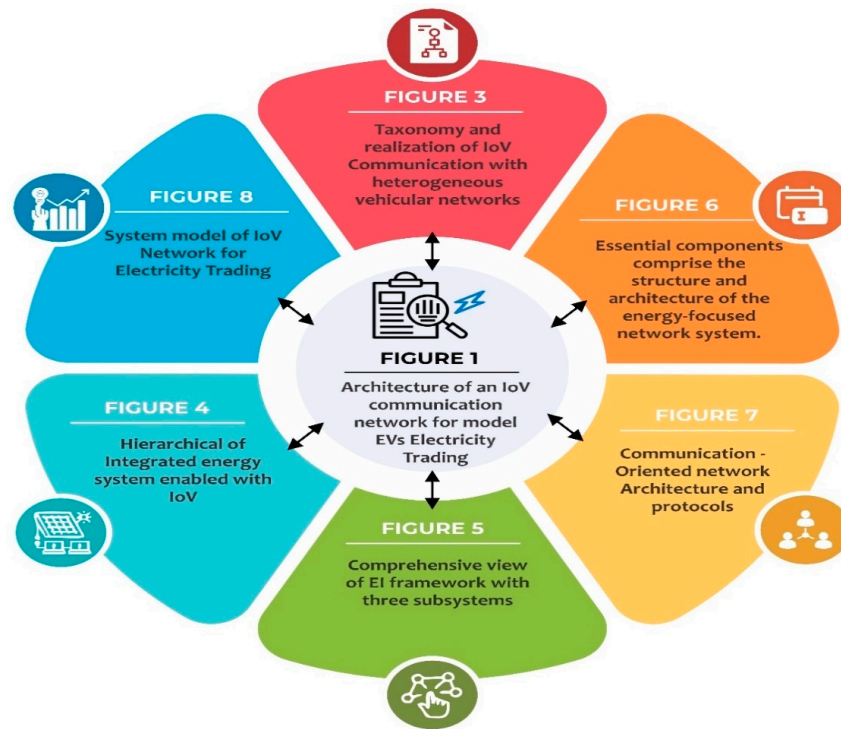


Figure 10. Integrated framework of IOV: a holistic view from architecture to communication.

### 2. Fitness function

When calculating an EV vendor index, we consider distance, energy consumption, and advertising expenditures. The following statement shows the fitness examination for optimization concerns:

$$Fitness = \left[ a \sum_{l=1}^p \ln(b + E_l^{req} P_i^s) + (1 - d_{i \leftarrow l}) \right]; E_l^{req} \leq E_l^{rt} \tag{13}$$

Here, the utility function of the  $j^{th}$  CS relies on the energy required and price announced by EVs, and thus, the utility function of the  $j^{th}$  CS is given by,

$$U_j = a_j \sum \ln(b_j + E_j^{req} P_i^s) \tag{14}$$

If the price announced by the  $i^{th}$  EV is expressed as  $P_i^s$  and revenue availability with the  $j^{th}$  CS is  $R_j$  such that ( $R_j > 0$ ), then the objective function can be given by,

$$O_j : \max_{\{E_j^{req}, \forall j \in J\}} U_j \tag{15}$$

### 3. Proposed TSOA

The trading is performed using the proposed TSOA, which is generated by adding the Taylor series and SOA. Here, the SOA [37] is a population-driven technique that involves two different justice principles, namely the equality of opportunity principle and the equality of community principle. This algorithm is very effective in solving economic dispatch problems and performs well on unconstrained and constrained functions. The Taylor series [38] describes the function of complicated attributes with several terms. The hybridization of both the Taylor series with SOA achieves efficient performance by resolving optimization problems. The proposed TSOA steps are as follows:

**Step 1. Initialization**

The preliminary step is initialization of the solution, which is expressed as  $F$ , where  $1 \leq \rho \leq \kappa$ .

$$F = \{F_1, F_2, \dots, F_\rho, \dots, F_\kappa\} \tag{16}$$

**Step 2. Determination of fitness**

The fitness has already been described in Section 4.1.1 using Equation (13).

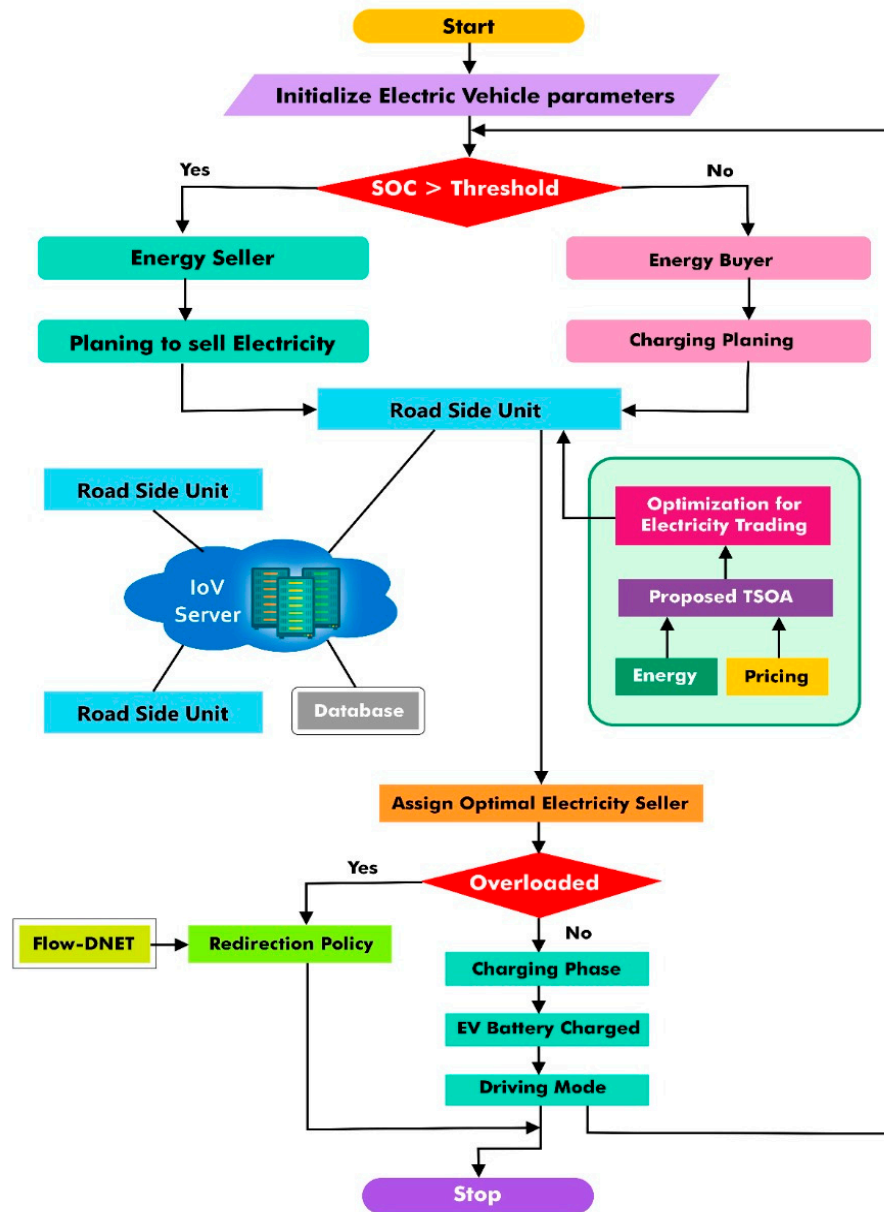


Figure 11. Proposed Taylor Social Optimization model algorithm flow with an optimal solution.

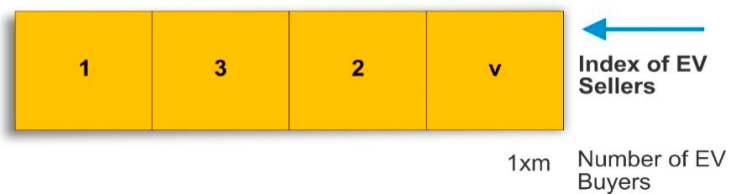


Figure 12. Representation of solution using proposed TSOA algorithm.

### Step 3. Evaluation of equality of opportunity

As per SOA [37], the equality of opportunity states that the consequent position of each entity is given by,

$$F_r^{new} = F_r^{old} + rand\left(X - Y \times F_r^{old}\right) \quad (17)$$

Here, the best position is given as,

$$X = rand\{S, A\} \quad (18)$$

The density point is given as,

$$A = \frac{F_1 z_1 + F_2 z_2 + \dots + F_0 z_0}{z_1 + z_2 + \dots + z_0} \quad (19)$$

Equation (17) can be expressed as,

$$F_r^{k+1} = F_r^k (1 - rand.Y) + rand.X \quad (20)$$

From the Taylor series [38],

$$F_r^{k+1} = F_r^k + \frac{F_r^{k'}}{1!} + \frac{F_r^{k''}}{2!} \quad (21)$$

Assume  $l = 1$  and substitute  $F_r^{k'}$  and  $F_r^{k''}$ ,

$$F_r^{k+1} = F_r^k + \frac{F_r^k - F_r^{k-1}}{1!} + \frac{F_r^k - 2F_r^{k-1} + F_r^{k-2}}{2!} \quad (22)$$

$$F_r^k = \frac{2}{5} \left[ F_r^{k+1} + 2F_r^{k-1} - \frac{F_r^{k-2}}{2} \right] \quad (23)$$

Substitute Equation (23) in Equation (20),

$$F_r^{k+1} = \frac{2}{5} \left[ F_r^{k+1} + 2F_r^{k-1} - \frac{F_r^{k-2}}{2} \right] (1 - rand.Y) + rand.X \quad (24)$$

$$F_r^{k+1} = \frac{2}{5} F_r^{k+1} (1 - rand.Y) + \frac{2}{5} 2F_r^{k-1} (1 - rand.Y) - \frac{2}{5} \frac{F_r^{k-2}}{2} (1 - rand.Y) + rand.X \quad (25)$$

The final update equation of the proposed TSOA is given as,

$$F_r^{k+1} = \frac{1}{3 + 2rand.Y} \left[ \left( 4F_r^{k-1} - F_r^{k-2} \right) (1 - rand.Y) + 5rand.X \right] \quad (26)$$

### Step 4. Evaluation of principle of community

Hence, the computation of the principle of community is expressed by,

$$F_r^{new} = F_r^{old} + rand(S - J) \quad (27)$$

Here, the empty point is expressed as,

$$J = \frac{F_1 \frac{1}{z_1} + F_2 \frac{1}{z_2} + \dots + F_0 \frac{1}{z_0}}{\frac{1}{z_1} + \frac{1}{z_2} + \dots + \frac{1}{z_0}} \quad (28)$$

### Step 5. Evaluation of density point and empty point

The density point is given as,

$$A = \sum_{l=1}^I \frac{z_l}{\sum_{r=1}^I z_r} F_l \quad (29)$$

The empty point is given as,

$$J = \sum_{l=1}^I \frac{\frac{1}{z_l}}{\sum_{r=1}^I \frac{1}{z_r}} F_l \quad (30)$$

The density points are given as,

$$A = \sum_{l=1}^I \hat{z}_l F_l \quad (31)$$

The empty points are given as,

$$J = \sum_{l=1}^I \tilde{z}_l F_l \quad (32)$$

Here,  $\hat{z}$  is given as,

$$\hat{z}_l = \frac{\frac{z_l}{e^{z_{\max}}}}{\sum_{r=1}^I \frac{z_r}{e^{z_{\max}}}} \quad (33)$$

Here,  $\tilde{z}$  is given as,

$$\tilde{z}_l = \frac{\frac{1}{e^{-z_{\max}}}}{\sum_{r=1}^I \frac{1}{e^{-z_{\max}}}} \quad (34)$$

### Step 6. Re-compute fitness for update solutions

The fitness of the update solutions is recalculated to obtain the best alternative for the best EV vendor selection.

### Step 7. Terminate

Up to the maximum number of iterations, we discover the optimal solutions repeatedly. The pseudocode of TSOA is illustrated in Algorithm 1.

## 4. Trading Algorithm

Here, energy trading is performed between EVs and CSs in the IoV network. The developed model considers various aspects like the capacity of EV batteries, the mobility of EVs, and pricing when making energy trading decisions. The method helps reduce the response time and improves the reliability of the network. The goal of energy supply in EVs is to make a profit, whereas for CSs, it is balancing the load. EVs move to CSs for either charging or discharging of their batteries. After reaching the CS, the final SoC of the CS and EV battery pool is changed. Each EV aims to acquire the maximum SoC level by charging the needed energy from the available CSs. The trading algorithm is depicted in Algorithm 2.

**Algorithm 1.** Pseudocode of proposed TSOAInput:  $F$ : Set of solutions,  $k$ : current iteration,  $k_{\max}$ : maximum iterationOutput: Best solution  $F^*$ 

Begin

Initialize random population  $F$ ;

Evaluate population;

 $X \leftarrow$  Best solution;For  $k = 1$  to  $k_{\max}$  do     $J \leftarrow$  Evaluate empty point;    For  $r = 1$  to  $I$  do         $E = \text{rand}(S, J)$ ;         $F = \text{rand}\{0, 1, 2\}$ ;        Compute  $F_r^{\text{new}}$  using Equation (26)

End

    If  $F_r^{\text{new}}$  better than  $F_r^{\text{old}}$  then         $F_r \leftarrow F_r^{\text{new}}$ 

End

Evaluate new population

 $S \leftarrow$  Best solution;     $A \leftarrow$  Compute Density point;    For  $r = 1$  to  $I$  do        Evaluate  $F_r^{\text{new}}$  using Equation (27)

End

    If  $F_r^{\text{new}}$  better than  $F_r^{\text{old}}$  then         $F_r \leftarrow F_r^{\text{new}}$ 

End

Evaluate new population

 $S \leftarrow$  Best solution;

End

Print best solution

**Algorithm 2.** Trading algorithmFor  $l = 1$  to  $p$  and  $l \neq i$ Compute  $SoC_l^{\text{prs}}$     If  $SoC_l^{\text{prs}} < SoC_l^{\text{thr}}$         Compute  $SoC_l^{\text{req}}$  and  $E_l^{\text{req}}$         Announce  $E_l^{\text{req}}$  to RSUs        For  $i = 1$  to  $p$  and  $i \neq l$             If  $SoC_i^{\text{prs}} > SoC_i^{\text{thr}}$                 Compute  $SoC_i^{\text{avl}}$  and  $E_i^{\text{avl}}$ 

End if

End for

End if

End for

Compute  $P_i^s$  and  $d_{i \leftarrow 1}$ For  $SoC_l^{\text{req}} < SoC_l^{\text{thr}}$ 

Call TSOA

    Draw  $E_l^{\text{req}}$  from corresponding EV's    Update  $SoC_i^{\text{upd}}$  and  $SoC_l^{\text{upd}}$ 

End for

**4.2. Flow Redirection Using Proposed Flow-DNET**

After electricity trading, the system performs flow redirection to evaluate the redirection factor for each RSU and determine if the CS is overloaded or underloaded. If the CS is overloaded, we utilize the Flow-DNET model to find the redirection policy. In this case, the trading is considered a failure. Thus, a broadcast message will be sent to neighboring

RSUs by the RSU. The neighboring RSU acknowledges the corresponding RSU by computing redirection factors, namely the load, number of EVs processed, distance, capacity, and delay.

Here, the load is given by,

$$L = \frac{\sum_{j=1}^n (X\mu_p + \lambda_j^{vehicle})}{\sum_{j=1}^n \lambda_j} \tag{35}$$

The distance is obtained from the mobility model, which has already been described in Section 3.2., and the capacity is the assumption.

The delay is obtained from the redirection model, which has already been described in Section 3.4.

Prediction of flow redirection priority using DBN

The flow redirection is predicted using a DBN [39]. Here, the input attributes like the load, capacity, number of EVs processed, distance, and delay are considered as inputs to the DBN. The structure of the DBN is revealed in Figure 13. One MLP layer and two RBM layers compose the DBN. The load, number of EVs managed, distance, capacity, and delay are the redirection factors that comprise the input for the first RBM in the DBN’s visible layer. The second RBM receives the output from the hidden layer and passes it on to the MLP.

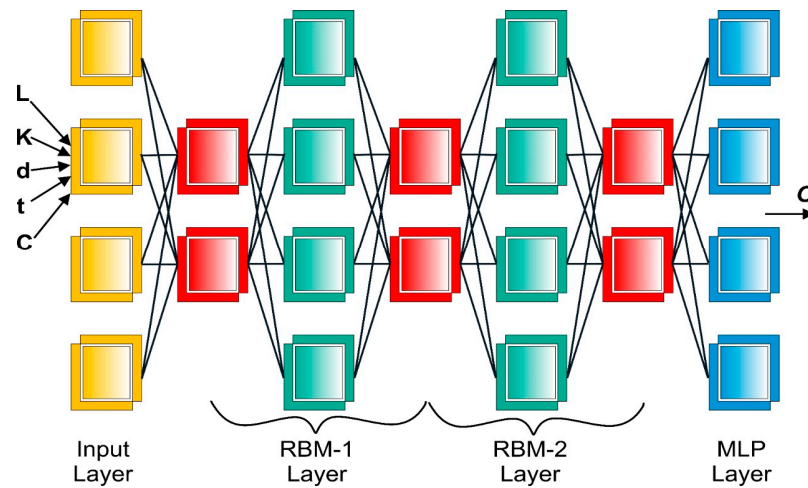


Figure 13. Structure of DBN.

The visible layer considers the load, capacity, number of EVs processed, distance, and delay as its input, and the hidden layer of the first RBM is given by,

$$f^1 = \{f_1^1, f_2^1, \dots, f_p^1, \dots, f_{10}^1\}; 1 \leq p \leq 10 \tag{36}$$

$$h^1 = \{h_1^1, h_2^1, \dots, h_l^1, \dots, h_q^1\}; 1 \leq l \leq q \tag{37}$$

The two biases linked to neurons amongst both layers for the first RBM are expressed as,

$$u^1 = \{u_1^1, u_2^1, \dots, u_p^1, \dots, u_{10}^1\} \tag{38}$$

$$v^1 = \{v_1^1, v_2^1, \dots, v_l^1, \dots, v_q^1\} \tag{39}$$

The weights from the first RBM are given by,

$$W^1 = \{W_{pl}^1\}; 1 \leq p \leq 10; 1 \leq l \leq q \tag{40}$$

where the weight vector size is given by  $10 \times q$ . Thus, the hidden layer output from the first RBM is provided with its bias and weights linked to each visible neuron and is expressed as,

$$h_l^1 = \sigma \left[ v_l^1 + \sum_p f_p^1 W_{pl}^1 \right] \quad (41)$$

Thus, the output generated from the first RBM is given by,

$$h^1 = \{h_l^1\}; 1 \leq l \leq q \quad (42)$$

Thus, the learning of the second RBM layer starts with the hidden layer output of the first one. The first RBM output is the visible layer input of the second RBM. Thus, the count of visible neurons is equal to the count of hidden neurons in the first RBM and is given by,

$$f^2 = \{f_1^2, f_2^2, \dots, f_q^2\} = \{h_l^1\}; 1 \leq l \leq q \quad (43)$$

The hidden layer of the second RBM is expressed as,

$$h^2 = \{h_1^2, h_2^2, \dots, h_l^2, \dots, h_q^2\}; 1 \leq l \leq q \quad (44)$$

For the second RBM, the weight vector is given by,

$$W^2 = \{W_{il}^2\}; 1 \leq l \leq q \quad (45)$$

The output of the  $l^{th}$  hidden neuron is given by,

$$h_l^2 = \sigma \left[ v_l^2 + \sum_p f_p^2 W_{il}^2 \right] \forall f_p^2 = h_l^1 \quad (46)$$

Hence, the output of the hidden layer generated is expressed as,

$$h^2 = \{h_l^2\}; 1 \leq l \leq q \quad (47)$$

The aforementioned equation establishes MLP input in which neurons count in the input layer as  $q$ . The MLP input layer is given by,

$$g = \{g_1, g_2, \dots, g_l, \dots, g_q\} = \{h_l^2\}; 1 \leq l \leq q \quad (48)$$

The MLP hidden layer is obtained by,

$$s = \{s_1, s_2, \dots, s_K, \dots, s_M\}; 1 \leq K \leq M \quad (49)$$

Consider  $X_K$  as the bias of the  $K^{th}$  hidden neuron in which  $K = 1, 2, \dots, M$ . The third layer represents the MLP output, which is given as,

$$o = \{o_1, o_2, \dots, o_r, \dots, o_z\}; 1 \leq r \leq z \quad (50)$$

MLP poses two weight vectors, one amongst the input layer and hidden layer, and the other amongst the hidden layer and output layer. Assume  $W^l$  is given by,

$$W^l = \{W_{IK}^l\}; 1 \leq l \leq q; 1 \leq K \leq M \quad (51)$$

The hidden layer output is given by,



$$s_K = \left[ \sum_{l=1}^q W_{lK}^I * g_l \right] X_K \forall g_l = h_l^2 \quad (52)$$

The weights amongst the hidden layer and output layer are expressed as,

$$W^H = \{ W_{Kr}^H \}; 1 \leq K \leq M; 1 \leq r \leq z \quad (53)$$

Hence, the output vector is evaluated with the weight and hidden layer output as,

$$o_r = \sum_{K=1}^M W_{Kr}^H * s_K \quad (54)$$

Thus, the output  $O$  is the priority level for RSU redirection where the priority is that the output to the RSU has maximum priority, and the flow will be redirected.

## 5. Results and Discussion

The efficiency of the TSOA-based Flow-DNET is evaluated considering pricing, fitness, and redirection success rate by altering rounds with 100, 150, 200, and 250 nodes. The TSOA-based Flow-DNET is run on a Windows 10 PC with 2 GB of RAM and an Intel core CPU using MATLAB 2020A [40].

### 5.1. Experimental Results

Figure 14 reveals the experimental results of the proposed TSOA-based Flow-DNET using 100 nodes and 150 nodes. The analysis with 100 nodes is displayed in Figure 14a. The analysis with 150 nodes is displayed in Figure 14b. Here, the red square represents the EV that moves towards the charging station.

### 5.2. Evaluation Measures

The created approach is modified by implementing some of the processes stated in Section 3. The evaluation metrics used for assessing the performance of the proposed TSOA-based Flow-DNET are fitness, pricing, and redirection success rate. The expressions for these measures have already been defined in Sections 3.3 and 3.4.

### 5.3. Comparative Methods

The techniques considered for the assessment of pricing includes Bayesian-Game-Based trading [4], DETF [17], PBFT [24], EVaaS [25], and the proposed TSOA + Flow-DNET.

The techniques taken for the assessment of the redirection success rate include Deep Reinforcement Learning [26], FORT [27], a control and regulation algorithm [28], and the proposed TSOA+ Flow-DNET.

### 5.4. Comparative Analysis

The assessment of the techniques using pricing, fitness, and the redirection success rate is described with 100, 150, 200, and 250 nodes.

#### 5.4.1. Assessment with 100 Nodes

Figure 15 depicts the assessment with 100 nodes and varied iterations. Figure 15a summarizes the fitness analysis findings. The suggested TSOA + Flow-DNET obtained a result of 0.109 after 101 repetitions. DETF, PBFT, EVaaS, and Bayesian-Game-Based Trading each received fitness ratings of 0.253, 0.138, 0.134, and 0.354, respectively. Furthermore, TSOA + Flow-DNET achieved a fitness measure of 0.013 for 451 iterations. Likewise, DETF, PBFT, Bayesian-Game-Based Trading, and EVaaS methods achieved fitness values as high as the proposed model. The analysis with pricing is shown in Figure 15b. For 101 iterations, the costs evaluated by Bayesian-Game-Based trading, DETF, PBFT, and EVaaS are 6.458%, 6.082%, 5.714%, and 8.100%, while that of the proposed TSOA + Flow-DNET is 5.000%.

Additionally, for 451 iterations, the pricings evaluated by Bayesian-Game-Based trading, DETF, PBFT, and EVaaS are 16%, 15.526%, 15.061%, and 17.260%, while that of the proposed TSOA + Flow-DNET is 14.160%. The analysis of the redirection success rate is revealed in Figure 15c. For 101 iterations, the redirection success rates evaluated by Deep Reinforcement Learning, FORT, and the control and regulation algorithm are 0.524, 0.533, and 0.570, while that of the proposed TSOA + Flow-DNET is 0.600. Moreover, for 451 iterations, the redirection success rates evaluated by Deep Reinforcement Learning, FORT, and the control and regulation algorithm are 0.672, 0.683, and 0.731, while that of the proposed TSOA + Flow-DNET is 0.769. The performance improvements of Deep Reinforcement Learning, FORT, and the control and regulation algorithm with respect to the proposed TSOA+ Flow-DNET using the redirection success rate are 12.613%, 11.183%, and 4.941%. From the analysis, it is concluded that our proposed TSOA + Flow-DNET achieved better performance than the existing model due to the effectiveness of the proposed system. This is because, in order to attain the best performance, the devised model adapted the optimization concept that aims to provide the optimal solution. Hence, the same performance was assessed by varying the nodes to 150, 200, and 250.

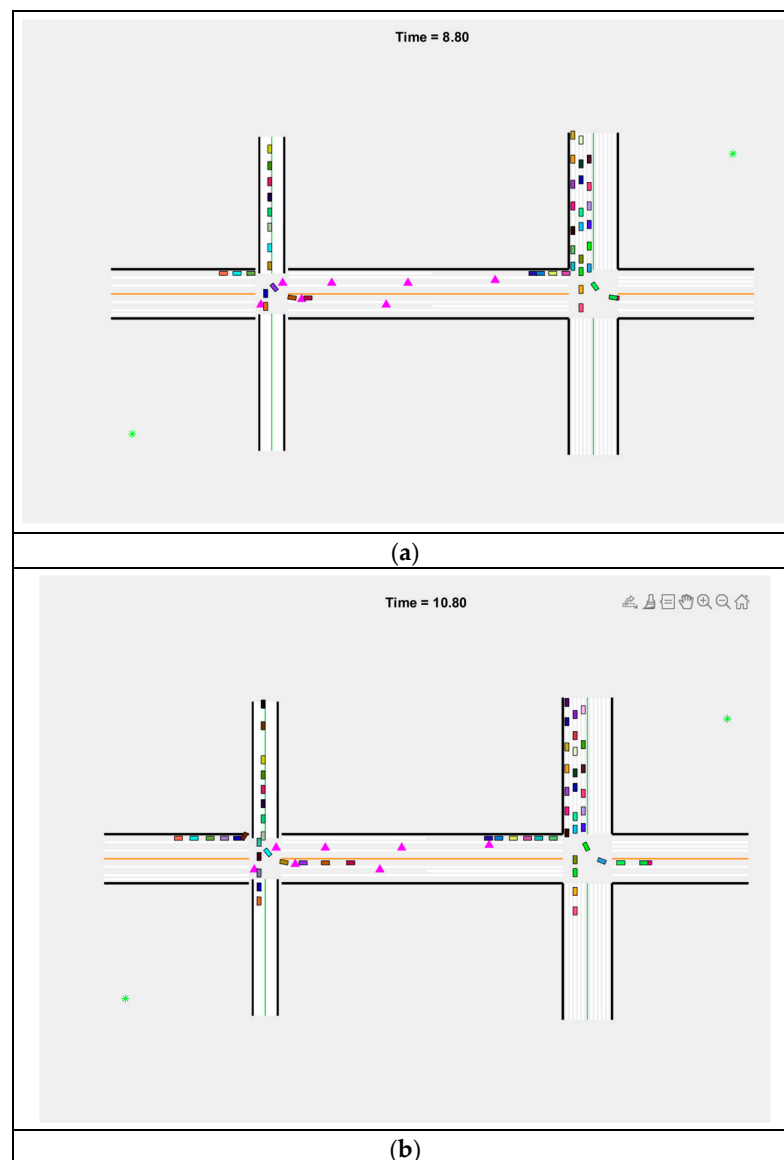


**Figure 14.** Experimental results of proposed TSOA-based Flow-DNET using (a) 100 nodes, (b) 150 nodes.

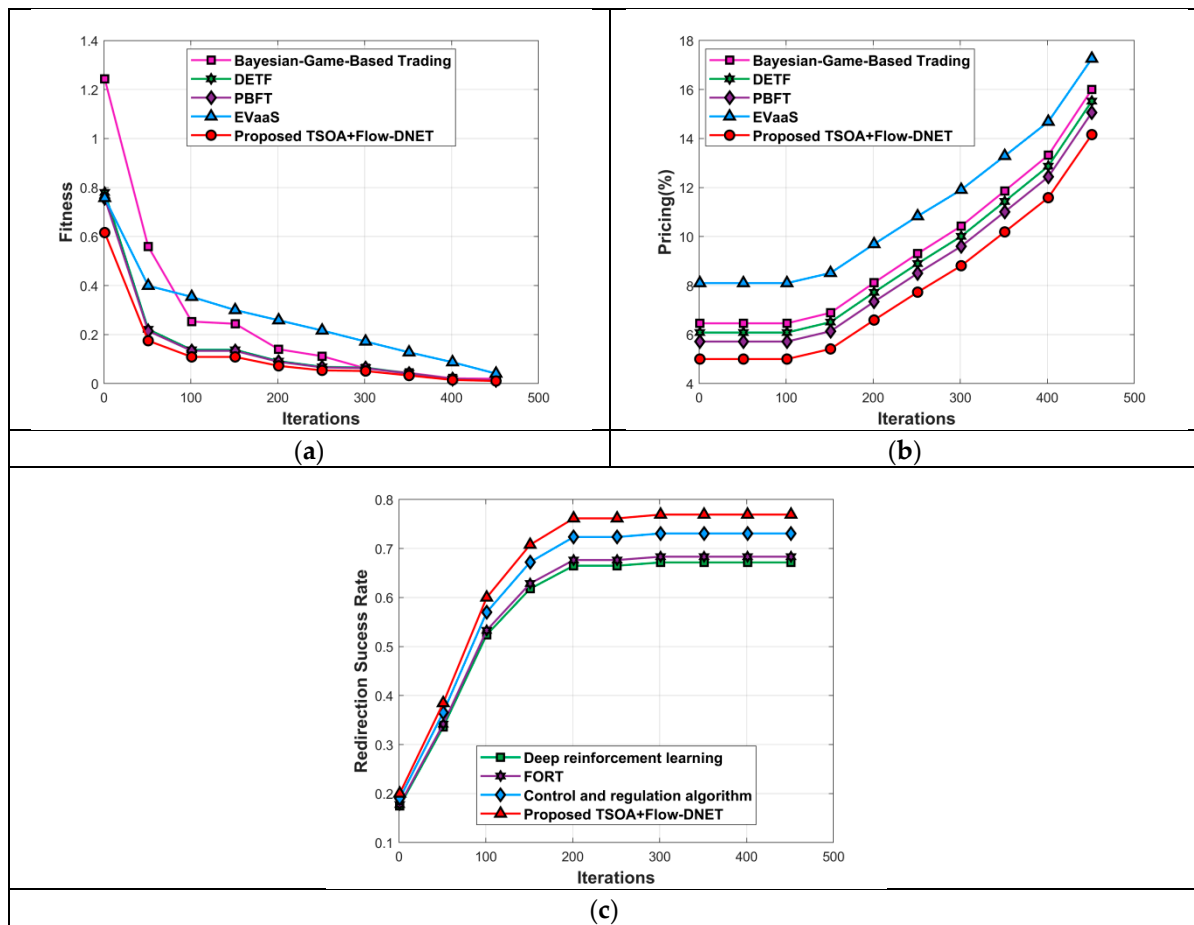


Figure 15. Assessment with 100 nodes using (a) fitness, (b) pricing, (c) redirection success rate.

#### 5.4.2. Assessment with 150 Nodes

Figure 16 represents the assessment with 150 nodes when altering the number of iterations. The analysis of fitness is revealed in Figure 16a. For 101 iterations, the fitness evaluated by Bayesian-Game-Based Trading is 0.439, DETF is 0.836, PBFT is 0.605, EVaaS is 0.437, and the proposed TSOA + Flow-DNET is 0.303. Additionally, for 451 iterations, the fitness evaluated by Bayesian game-based trading is 0.437, DETF is 0.352, PBFT is 0.603, and EVaaS is 0.437, and the proposed TSOA + Flow-DNET is 0.301. The analysis with pricing is shown in Figure 16b. For 101 iterations, the pricing evaluated by Bayesian-Game-Based Trading is 11.488%, DETF is 9.143%, PBFT is 5.065%, EVaaS is 7.690%, and the proposed TSOA + Flow-DNET is 2.400%. Moreover, for 451 iterations, the pricing evaluated by Bayesian-Game-Based Trading is 26.432%, DETF is 24.087%, PBFT is 18.562%, EVaaS is 22.118%, and the proposed TSOA + Flow-DNET is 14.953%. The analysis of the redirection success rate is revealed in Figure 16c. For 101 iterations, the redirection success rate evaluated by Deep Reinforcement Learning is 0.547, FORT is 0.559, the control and regulation algorithm is 0.584, and the proposed TSOA+ Flow-DNET is 0.621. Additionally, for 451 iterations, the redirection success rate evaluated by Deep Reinforcement Learning is 0.713, FORT is 0.729, the control and regulation algorithm is 0.762, and the proposed TSOA+ Flow-DNET is 0.810. The performance improvements of Deep Reinforcement Learning, FORT, and the control, and regulation algorithm with respect to the proposed TSOA+ Flow-DNET using redirection success rates are 11.975%, 10%, and 5.925%, respectively.

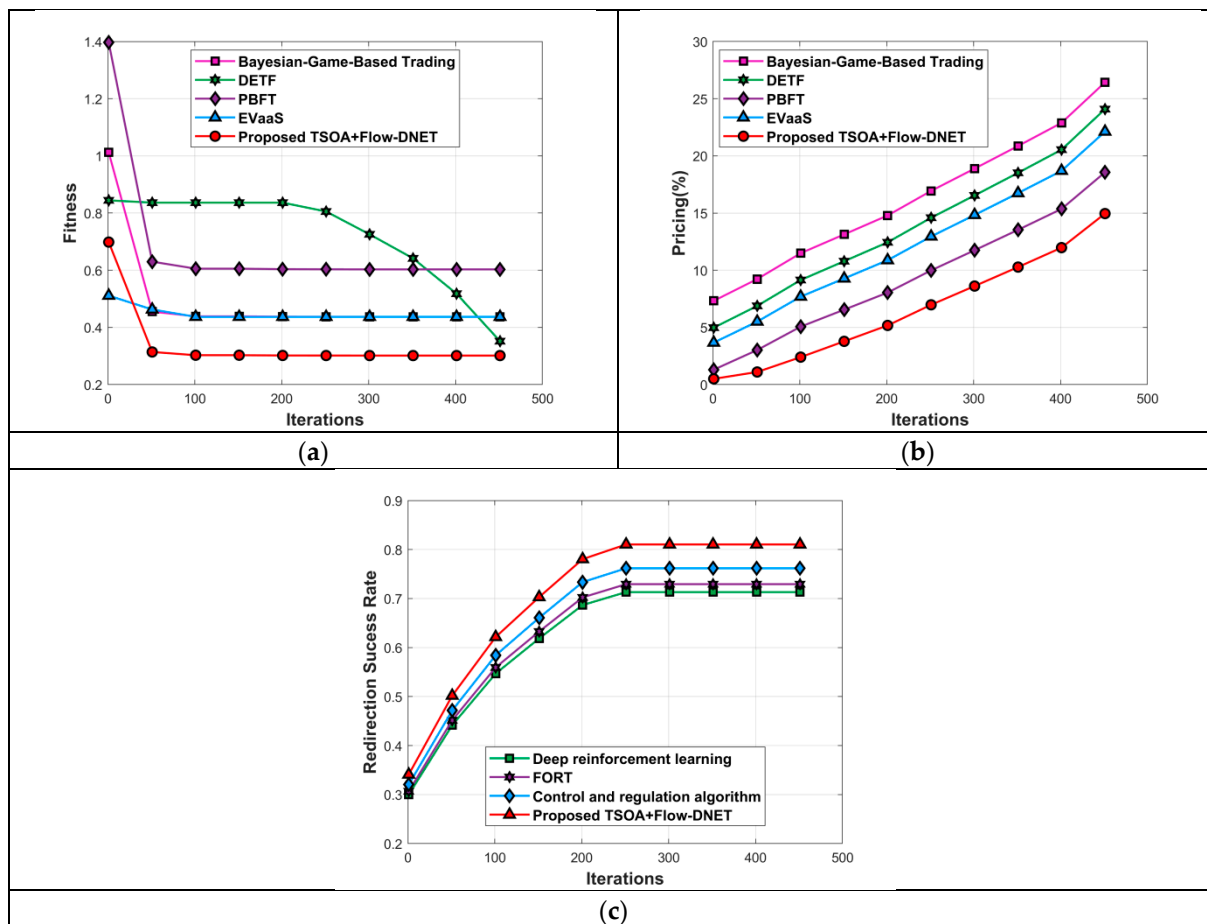


Figure 16. Assessment with 150 nodes using (a) fitness, (b) pricing, (c) redirection success rate.

### 5.4.3. Assessment with 200 Nodes

Figure 17 presents the assessment with 200 nodes when altering the number of iterations. The analysis of fitness is revealed in Figure 17a. For 101 iterations, the smallest fitness of 0.014 is evaluated by the proposed TSOA + Flow-DNET, while the fitness values of Bayesian game-based trading, DETF, PBFT, and EVaaS are 0.028, 0.020, 0.054, and 0.036. Additionally, for 451 iterations, the smallest fitness of 0 is evaluated by the proposed TSOA + Flow-DNET, while the fitness value of Bayesian game-based trading, DETF, PBFT, and EVaaS is 0 for each. The analysis with pricing is shown in Figure 17b. For 101 iterations, the lowest pricing of 13.669% is evaluated by the proposed TSOA + Flow-DNET, while the pricings measured by Bayesian-Game-Based Trading, DETF, PBFT, and EVaaS are 16.537%, 16.875%, 15.894%, and 15.358%. Moreover, for 451 iterations, the lowest pricing of 20.074% is evaluated by the proposed TSOA + Flow-DNET, while the pricings evaluated by Bayesian-Game-Based Trading, DETF, PBFT, and EVaaS are 24.287%, 24.782%, 23.341%, and 22.555%. The analysis of the redirection success rate is shown in Figure 17c. For 101 iterations, the biggest redirection success rate of 0.714 is evaluated by the proposed TSOA+ Flow-DNET, while the redirection success rates evaluated by Deep Reinforcement Learning, FORT, and the control and regulation algorithm are 0.635, 0.656, and 0.676. In addition, for 451 iterations, the biggest redirection success rate of 0.918 is evaluated by the proposed TSOA+ Flow-DNET, while the redirection success rates evaluated by Deep Reinforcement Learning, FORT, and the control and regulation algorithm are 0.816, 0.844, and 0.869. The performance improvements of Deep Reinforcement Learning, FORT, and the control and regulation algorithms with respect to the proposed TSOA+ Flow-DNET using redirection success rates are 11.111%, 8.061%, and 5.337%.

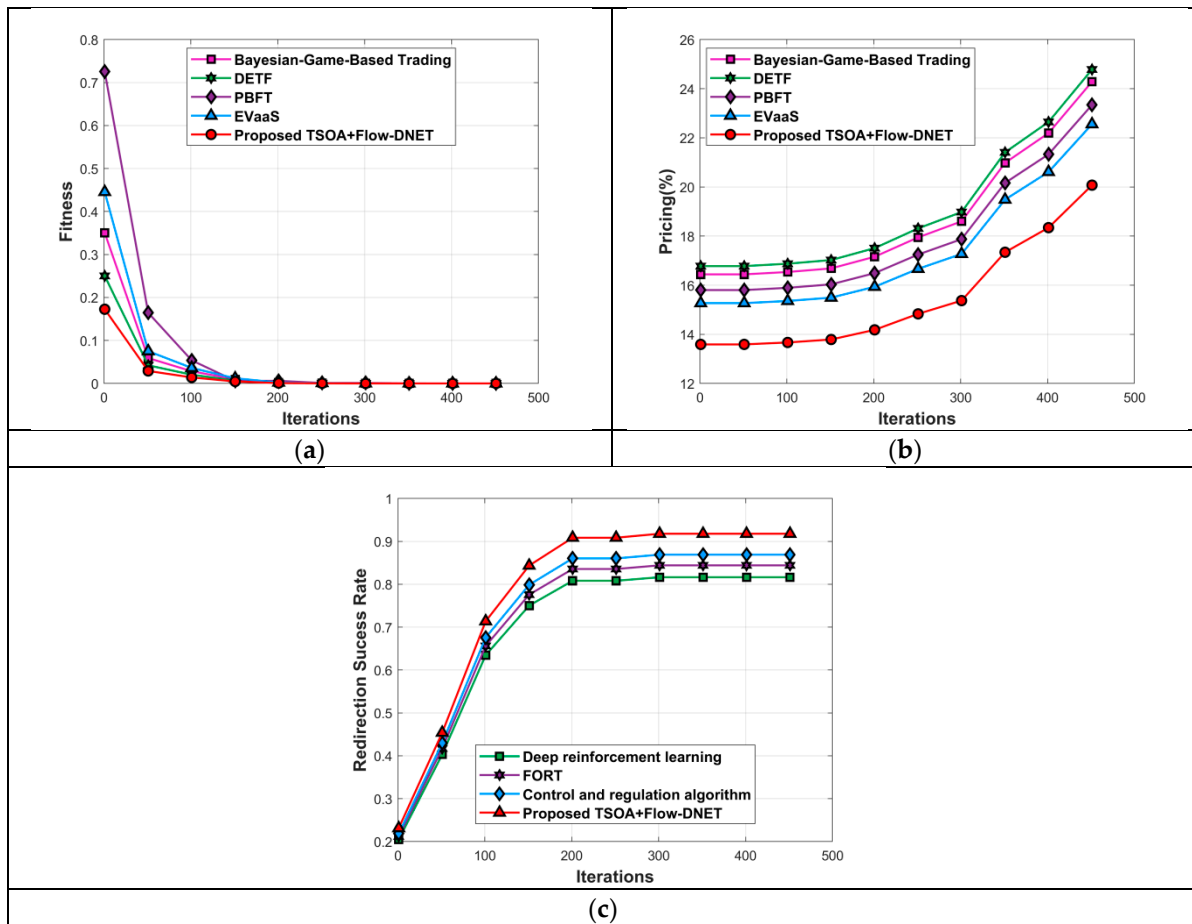
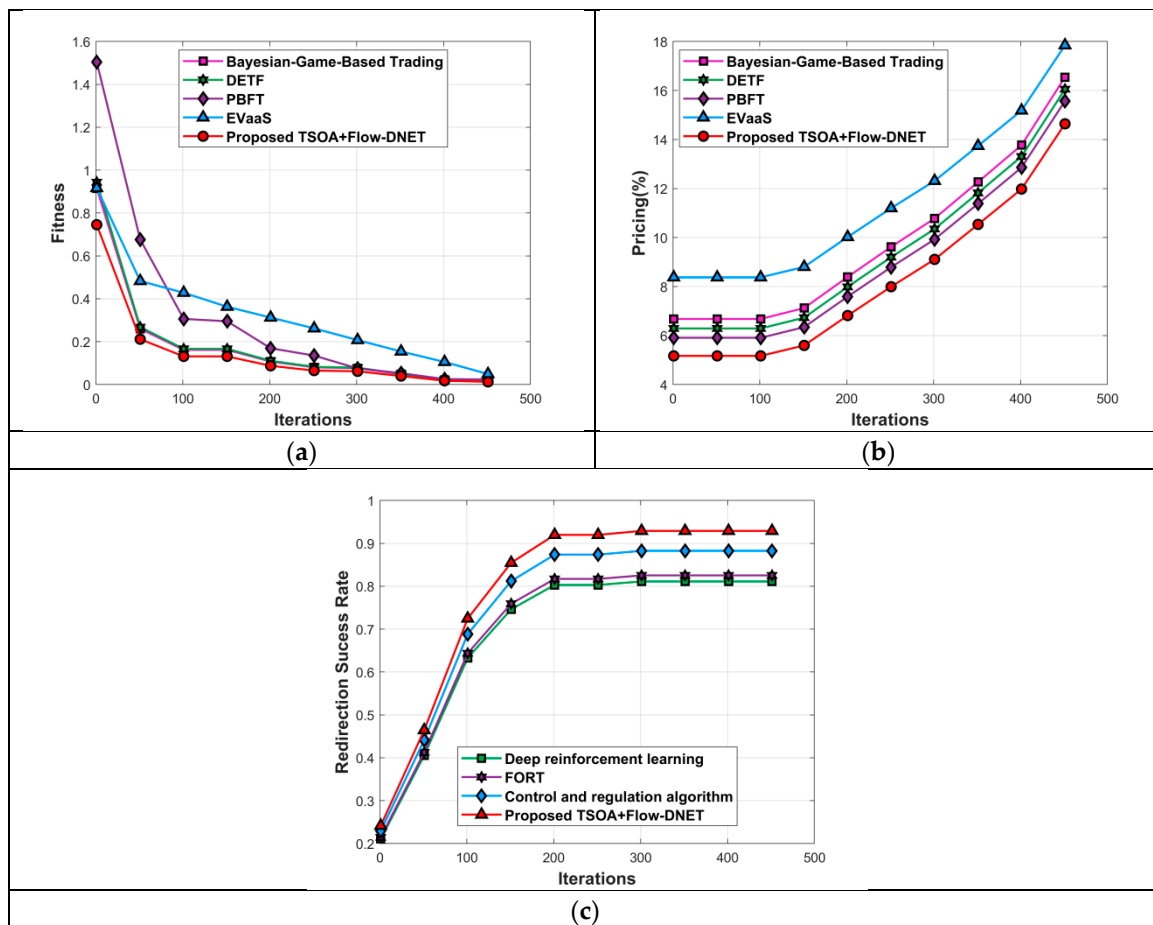


Figure 17. Assessment with 200 nodes using (a) fitness, (b) pricing, (c) redirection success rate.

#### 5.4.4. Assessment with 250 Nodes

Figure 18 presents the assessment with 250 nodes when altering the number of iterations. The analysis of fitness is revealed in Figure 18a. For 101 iterations, the fitness values evaluated by Bayesian game-based trading, DETF, PBFT, EVaaS, and the proposed TSOA + Flow-DNET are 0.162, 0.167, 0.306, 0.428, and 0.132. Moreover, for 451 iterations, the fitness values evaluated by Bayesian game-based trading, DETF, PBFT, EVaaS, and the proposed TSOA + Flow-DNET are 0.016, 0.016, 0.024, 0.049, and 0.013. The analysis of pricing is revealed in Figure 18b. For 101 iterations, the pricings evaluated by Bayesian game-based trading, DETF, PBFT, EVaaS, and the proposed TSOA + Flow-DNET are 6.678%, 6.289%, 5.909%, 8.375%, and 5.170%. Additionally, for 451 iterations, the pricings evaluated by Bayesian game-based trading, DETF, PBFT, EVaaS, and the proposed TSOA + Flow-DNET are 16.544%, 16.053%, 15.573%, 17.847%, and 14.641%. The analysis of the redirection success rate is shown in Figure 18c. For 101 iterations, the redirection success rates evaluated by Deep Reinforcement Learning, FORT, the control and regulation algorithm, and the proposed TSOA+ Flow-DNET are 0.633, 0.644, 0.688, and 0.725. In addition, for 451 iterations, the redirection success rates evaluated by Deep Reinforcement Learning, FORT, the control and regulation algorithm, and the proposed TSOA+ Flow-DNET are 0.811, 0.825, 0.883, and 0.929. The performance improvements of Deep Reinforcement Learning, FORT, and the control, and regulation algorithm with respect to the proposed TSOA+ Flow-DNET using redirection success rates are 12.701%, 11.194%, and 4.951%, respectively.



**Figure 18.** Assessment with 250 nodes using (a) fitness, (b) pricing, (c) redirection success rate.

### 5.5. Comparative Discussion

In this section, the analysis is carried out for two processes, pricing and the redirection success rate. To analyze the performance of pricing, the existing models, such as Bayesian-Game-Based trading, DETF, PBFT, and EVaaS, have been considered. Here, the analysis is performed by increasing the number of nodes from 100 to 250 with four equal divisions since the performance should vary when changing the setup. Table 2 shows the results of the comparative test, which prioritized cost and fitness. DETF, PBFT, EVaaS, and Bayesian game-based trading had fitness ratings of 0.020, 0.013, 0.041, and 0.011, respectively, out of all the evaluated techniques. At 0.011, the TSOA + Flow-DNET algorithm has the lowest fitness value. The algorithm performs best with 100 nodes. The TSOA + Flow-DNET plan costs USD 14,160,000, including PBFT at 15.061 percent, DETF at 15.526 percent, and EVaaS at 17.26 percent. The CS and EV exchange energy to optimize their financial benefits since their owners control their pricing. The TSOA + Flow-DNET model calculates a maximum price of 14.953% and a minimum fitness value of 0.301 using a network of 150 nodes. The TSOA + Flow-DNET architecture achieves a minimal fitness of 0 and an optimum cost of 0.816% with 200 nodes. When using 250 nodes, the suggested TSOA + Flow-DNET achieves the highest cost of 14.641% and the lowest fitness of 0.013.

To analyze the performance of pricing, the existing models, such as Deep Reinforcement Learning, FORT, and the control and regulation algorithm, have been considered. Here, the analysis is performed by increasing the number of nodes by the order of 100 nodes, 150 nodes, 200 nodes, and 250 nodes since the performance should vary when modifying the experimental setup. Table 3 presents the assessment of techniques with redirection success rates by altering iterations. Using 100 nodes, the highest redirection success rate of 0.769 is measured by the proposed TSOA + Flow-DNET, while the redirec-

tion success rates of Deep Reinforcement Learning, FORT, and the control and regulation algorithm are 0.672, 0.683, and 0.731. The highest redirection success rate is measured by the proposed TSOA+ Flow-DNET, which reveals faster and more effective trip speeds. Using 150 nodes, the highest redirection success rate of 0.810 is measured by the proposed TSOA + Flow-DNET. Using 200 nodes, the highest redirection success rate of 0.918 is measured by the proposed TSOA+ Flow-DNET. Using 250 nodes, the highest redirection success rate of 0.929 is measured by the proposed TSOA+ Flow-DNET.

**Table 2.** Comparative analysis.

Nodes	Metrics	Bayesian-Game-Based Trading	DETF	PBFT	EVaaS	Proposed TSOA + Flow-DNET
100 nodes	Fitness	0.020	0.013	0.013	0.041	0.011
	Pricing (%)	16.000	15.526	15.061	17.260	14.160
150 nodes	Fitness	0.437	0.352	0.603	0.437	0.301
	Pricing (%)	26.432	24.087	18.562	22.118	14.953
200 nodes	Fitness	0	0	0	0	0
	Pricing (%)	0.816	0.844	0.869	0.918	0.816
250 nodes	Fitness	0.016	0.016	0.024	0.049	0.013
	Pricing (%)	16.544	16.053	15.573	17.847	14.641

**Table 3.** Analysis with redirection success rate.

Nodes	Deep Reinforcement Learning	FORT	Control and Regulation Algorithm	Proposed TSOA + Flow-DNET
100 nodes	0.672	0.683	0.731	0.769
150 nodes	0.713	0.729	0.762	0.810
200 nodes	0.816	0.844	0.869	0.918
250 nodes	0.811	0.825	0.883	0.929

### 5.6. Analysis Based on Computational Time

Table 4 shows the analysis based on the computational time. This table shows the computational time of the proposed method is lower than other comparative methods.

**Table 4.** Analysis based on computational time.

Methods	Computational Time (mins)
Setup 1	
Bayesian-Game-Based trading	8.782346782569
DETF	7.846758264756
PBFT	6.893748641209
EVaaS	5.08784675123
Proposed TSOA + Flow-DNET	4.56913749103
Setup 2	
Deep Reinforcement Learning	7.03256645632
FORT	6.64893573894
Control and regulation algorithm	5.09277364751
Proposed TSOA+ Flow-DNET	4.673648735687

## 6. Conclusions

An approach is developed for optimum electricity trading with a deep flow redirection mechanism in the IoV, considering the Flow-DNET model. Here, four entities are adapted that include EVs, auctioneers, RSUs, and the IoV server. In the electrical market, electric vehicles act as energy consumers, putting demands on power providers, or RSUs. Afterwards, an auctioneer supervises these providers as they participate in auctions. The auction process is constructed using a recently developed optimization approach called TSOA, which takes into account the fitness function. A novel approach to energy and cost analysis identifies the most beneficial exercise models for charging stations. In addition, we obtain the proposed TSOA by combining the ideas of the Taylor series and the Social Optimization Algorithm. The redirection of flow is carried out after the electricity trade. As per the analysis carried out for both pricing and the redirection success rate, the proposed TSOA + Flow-DNET achieved better performance than the existing models. Here, the redirection factor is computed for each RSU to make a decision regarding the overloading or under loading conditions of the CS. If the CS is overloaded, the Flow-DNET model is used to find the redirection policy. The proposed TSOA + Flow-DNET provided enhanced efficiency with the smallest pricing of 0.816% and the highest redirection success rate of 0.918. In the future, other advanced optimization techniques can be adapted to check the feasibility of the developed model.

**Author Contributions:** R.S.: conceptualization, methodology, validation, formal analysis, investigation, resource gathering, data curation, writing—original draft preparation, and visualization. P.K.: conceptualization, supervision, resource gathering, visualization, data curation, validation, and formal analysis. R.M.E.: methodology, validation, and writing—review and editing. G.M.S.: methodology, validation, and writing—review and editing. All authors have read and agreed to the published version of the manuscript.

**Funding:** This research received no external funding.

**Data Availability Statement:** No new data were created or analyzed in this study. Data sharing is not applicable to this article.

**Conflicts of Interest:** The authors declare no conflicts of interest.

## References

1. Ušinskis, V.; Makulavičius, M.; Petkevičius, S.; Dzedzickis, A.; Bučinskas, V. Towards Autonomous Driving: Technologies and Data for Vehicles-to-Everything Communication. *Sensors* **2024**, *24*, 3411. [[CrossRef](#)] [[PubMed](#)]
2. Xu, Y.; Alderete Peralta, A.; Balta-Ozkan, N. Vehicle-to-Vehicle Energy Trading Framework: A Systematic Literature Review. *Sustainability* **2024**, *16*, 5020. [[CrossRef](#)]
3. Liu, P.; Wang, C.; Hu, J.; Fu, T.; Cheng, N.; Zhang, N.; Shen, X. Joint Route Selection and Charging Discharging Scheduling of EVs in V2G Energy Network. *IEEE Trans. Veh. Technol.* **2020**, *69*, 10630–10641. [[CrossRef](#)]
4. Xia, S.; Lin, F.; Chen, Z.; Tang, C.; Ma, Y.; Yu, X. A Bayesian Game Based Vehicle-to-Vehicle Electricity Trading Scheme for Blockchain-Enabled Internet of Vehicles. *IEEE Trans. Veh. Technol.* **2020**, *69*, 6856–6868. [[CrossRef](#)]
5. Wang, J.; Jiang, C.; Han, Z.; Ren, Y.; Hanzo, L. Internet of Vehicles: Sensing-Aided Transportation Information Collection and Diffusion. *IEEE Trans. Veh. Technol.* **2018**, *67*, 3813–3825. [[CrossRef](#)]
6. Yang, F.; Wang, S.; Li, J.; Liu, Z.; Sun, Q. An overview of Internet of Vehicles. *China Commun.* **2014**, *11*, 1–15. [[CrossRef](#)]
7. Lim, W.Y.B.; Huang, J.; Xiong, Z.; Kang, J.; Niyato, D.; Hua, X.S.; Leung, C.; Miao, C. Towards Federated Learning in UAV-Enabled Internet of Vehicles: A Multi-Dimensional Contract-Matching Approach. *IEEE Trans. Intell. Transp. Syst.* **2021**, *22*, 5140–5154. [[CrossRef](#)]
8. Florian, M.; Finster, S.; Baumgart, I. Privacy-preserving cooperative route planning. *IEEE Internet Things J.* **2014**, *1*, 590–599. [[CrossRef](#)]
9. Kumar, P.M.; Devi, G.U.; Manogaran, G.; Sundarasekar, R.; Chilamkurti, N.; Varatharajan, R. Ant colony optimization algorithm with Internet of Vehicles for intelligent traffic control system. *Comput. Netw.* **2018**, *144*, 154–162. [[CrossRef](#)]
10. Lopes, J.A.P.; Soares, F.J.; Almeida, P.M.R. Integration of electric vehicles in the electric power system. *Proc. IEEE* **2011**, *99*, 168–183. [[CrossRef](#)]
11. Abbas, F.; Feng, D.; Habib, S.; Rasool, A.; Numan, M. An Improved Optimal Forecasting Algorithm for Comprehensive Electric Vehicle Charging Allocation. *Energy Technol.* **2019**, *7*, 1900436. [[CrossRef](#)]



12. Majidpour, M.; Qiu, C.; Chu, P.; Gadh, R.; Pota, H.R. Fast prediction for sparse time series: Demand forecast of EV charging stations for cell phone applications. *IEEE Trans. Ind. Inform.* **2015**, *11*, 242–250. [[CrossRef](#)]
13. Chiş, A.; Lundén, J.; Koivunen, V. Reinforcement learning-based plug-in electric vehicle charging with forecasted price. *IEEE Trans. Veh. Technol.* **2017**, *66*, 3674–3684. [[CrossRef](#)]
14. Ma, W.J.; Gupta, V.; Topcu, U. Distributed Charging Control of Electric Vehicles Using Online Learning. *IEEE Trans. Autom. Control.* **2017**, *62*, 5289–5295. [[CrossRef](#)]
15. Saputra, Y.M.; Nguyen, D.N.; Hoang, D.T.; Vu, T.X.; Dutkiewicz, E.; Chatzinotas, S. Federated Learning Meets Contract Theory: Economic-Efficiency Framework for Electric Vehicle Networks. *IEEE Trans. Mob. Comput.* **2022**, *21*, 2803–2817. [[CrossRef](#)]
16. Liu, T.; Hu, X. A Bi-Level Control for Energy Efficiency Improvement of a Hybrid Tracked Vehicle. *IEEE Trans. Ind. Inform.* **2018**, *14*, 1616–1625. [[CrossRef](#)]
17. Said, D. A Decentralized Electricity Trading Framework (DETF) for Connected EVs: A Blockchain and Machine Learning for Profit Margin Optimization. *IEEE Trans. Ind. Inform.* **2021**, *17*, 6594–6602. [[CrossRef](#)]
18. Aledhari, M.; Pierro MDi Hefeida, M.; Saeed, F. A Deep Learning-Based Data Minimization Algorithm for Fast and Secure Transfer of Big Genomic Datasets. *IEEE Trans. Big Data* **2018**, *7*, 271–284. [[CrossRef](#)]
19. Kaiwartya, O.; Abdullah, A.H.; Cao, Y.; Altameem, A.; Prasad, M.; Lin, C.T.; Liu, X. Internet of Vehicles: Motivation, Layered Architecture, Network Model, Challenges, and Future Aspects. *IEEE Access* **2016**, *4*, 5356–5373. [[CrossRef](#)]
20. Bagga, P.; Das, A.K.; Wazid, M.; Rodrigues, J.J.P.C.; Park, Y. Authentication protocols in internet of vehicles: Taxonomy, analysis, and challenges. *IEEE Access* **2020**, *8*, 54314–54344. [[CrossRef](#)]
21. Al-Omais, H.; Sundararajan, E.A.; Alsaqour, R.; Abdullah, N.F.; Abdelhaq, M. A survey of data dissemination schemes in vehicular named data networking. *Veh. Commun.* **2021**, *30*, 100353. [[CrossRef](#)]
22. Wu, Y.; Wu, Y.; Guerrero, J.M.; Vasquez, J.C. A comprehensive overview of framework for developing sustainable energy internet: From things-based energy network to services-based management system. *Renew. Sustain. Energy Rev.* **2021**, *150*, 111409. [[CrossRef](#)]
23. Chen, C.; Zeng, Y.; Li, H.; Liu, Y.; Wan, S. A Multihop Task Offloading Decision Model in MEC-Enabled Internet of Vehicles. *IEEE Internet Things J.* **2023**, *10*, 3215–3230. [[CrossRef](#)]
24. Chen, X.; Zhang, X. Secure Electricity Trading and Incentive Contract Model for Electric Vehicle Based on Energy Blockchain. *IEEE Access* **2019**, *7*, 178763–178778. [[CrossRef](#)]
25. Aujla, G.S.; Jindal, A.; Kumar, N. EVaaS: Electric vehicle-as-a-service for energy trading in SDN-enabled smart transportation system. *Comput. Netw.* **2018**, *143*, 247–262. [[CrossRef](#)]
26. Ning, Z.; Dong, P.; Wang, X.; Guo, L.; Rodrigues, J.J.P.C.; Kong, X.; Huang, J.; Kwok, R.Y.K. Deep Reinforcement Learning for Intelligent Internet of Vehicles: An Energy-Efficient Computational Offloading Scheme. *IEEE Trans. Cogn. Commun. Netw.* **2019**, *5*, 1060–1072. [[CrossRef](#)]
27. Wang, X.; Ning, Z.; Wang, L. Offloading in Internet of Vehicles: A Fog-Enabled Real-Time Traffic Management System. *IEEE Trans. Ind. Inform.* **2018**, *14*, 4568–4578. [[CrossRef](#)]
28. Merhy, G.; Nait-Sidi-Moh, A.; Moubayed, N. Control, Regulation, and Optimization of Electric Vehicles' Reversible Energy Flows through an Energy Management Strategy 1 Control, Regulation and Optimization of Bidirectional Energy Flows for Electric Vehicles' Charging and Discharging. *Sustain. Cities Soc.* **2020**, *57*, 102129. [[CrossRef](#)]
29. Liu, R.; Liu, A.; Qu, Z.; Xiong, N.N. An UAV-Enabled Intelligent Connected Transportation System With 6G Communications for Internet of Vehicles. *IEEE Trans. Intell. Transp. Syst.* **2023**, *24*, 2045–2059. [[CrossRef](#)]
30. Sun, G.; Dai, M.; Zhang, F.; Yu, H.; Du, X.; Guizani, M. Blockchain-Enhanced High-Confidence Energy Sharing in Internet of Electric Vehicles. *IEEE Internet Things J.* **2020**, *7*, 7868–7882. [[CrossRef](#)]
31. Devendiran, R.; Kasinathan, P.; Ramchandaramurthy, V.K.; Subramaniam, U.; Govindarajan, U.; Fernando, X. Intelligent optimization for charging scheduling of electric vehicle using exponential Harris Hawks technique. *Int. J. Intell. Syst.* **2021**, *36*, 5816–5844. [[CrossRef](#)]
32. Turukmane, A.V.; Devendiran, R. M-MultiSVM: An Efficient Feature Selection Assisted Network Intrusion Detection System using Machine Learning. *Comput. Secur.* **2023**, *137*, 103587. [[CrossRef](#)]
33. Rajamoorthy, R.; Arunachalam, G.; Kasinathan, P.; Devendiran, R.; Ahmadi, P.; Pandiyan, S.; Muthusamy, S.; Panchal, H.; Kazem, H.A.; Sharma, P. A novel intelligent transport system charging scheduling for electric vehicles using Grey Wolf Optimizer and Sail Fish Optimization algorithms. *Energy Sources, Part A Recover. Util. Environ. Eff.* **2022**, *44*, 3555–3575. [[CrossRef](#)]
34. Zhang, Y.; Chen, J.; You, T.; Zhang, Y.; Liu, Z.; Du, C. Energy-Aware Optimization of Connected and Automated Electric Vehicles Considering Vehicle-Traffic Nexus. *IEEE Trans. Ind. Electron.* **2024**, *71*, 282–293. [[CrossRef](#)]
35. Safavat, S.; Rawat, D.B. Improved Multiresolution Neural Network for Mobility-Aware Security and Content Caching for Internet of Vehicles. *IEEE Internet Things J.* **2023**, *10*, 17813–17823. [[CrossRef](#)]
36. Cao, Y.; Kaiwartya, O.; Zhuang, Y.; Ahmad, N.; Sun, Y.; Lloret, J. A Decentralized Deadline-Driven Electric Vehicle Charging Recommendation. *IEEE Syst. J.* **2019**, *13*, 3410–3421. [[CrossRef](#)]
37. Karimi, N.; Khandani, K. Social optimization algorithm with application to economic dispatch problem. *Int. Trans. Electr. Energy Syst.* **2020**, *30*, e12593. [[CrossRef](#)]
38. AlameluMangai, S.; Sankar, B.R.; Alagarsamy, K. Taylor Series Prediction of Time Series Data with Error Propagated by Artificial Neural Network. *Int. J. Comput. Appl.* **2014**, *89*, 41–47. [[CrossRef](#)]

39. Teoh, E.J.; Tan, K.C.; Xiang, C. Estimating the number of hidden neurons in a feedforward network using the singular value decomposition. *IEEE Trans. Neural Netw.* **2006**, *17*, 1623–1629. [[CrossRef](#)]
40. Min, G.; Du, Y.; Wu, J.; Yan, S. Simulation Study of Mixed Traffic in China—A Practice in Beijing. In Proceedings of the 11th International IEEE Conference on Intelligent Transportation Systems, Beijing, China, 12–15 October 2008; pp. 281–285.

**Disclaimer/Publisher’s Note:** The statements, opinions and data contained in all publications are solely those of the individual author(s) and contributor(s) and not of MDPI and/or the editor(s). MDPI and/or the editor(s) disclaim responsibility for any injury to people or property resulting from any ideas, methods, instructions or products referred to in the content.